Prepared for
GEORGE C. MARSHALL SPACE FLIGHT CENTER
Huntsville Alabama

LOCATION OF PATTERN-DISTURBING STRUCTURES IN THE VICINITY OF AN ANTENNA

Final Report
Contract NAS8-5412
September 15, 1966

by

Dr. Harold Mott
Professor of Electrical Engineering
Project Director

Dr. Joseph C. Dowdle
Professor of Electrical Engineering
Project Co-Director

Mr. James E. Dudgeon
Research Associate

BUREAU OF ENGINEERING RESEARCH

BER

COLLEGE OF ENGINEERING

UNIVERSITY OF ALABAMA

UNIVERSITY ALABAMA

University of Alabama
Bureau of Engineering Research
University, Alabama

LOCATION OF PATTERN-DISTURBING STRUCTURES IN THE VICINITY OF AN ANTENNA

Final Report
Contract NAS8-5412
September 15, 1966

by

Dr. Harold Mott
Professor of Electrical Engineering
Project Director

Dr. Joseph C. Dowdle
Professor of Electrical Engineering
Project Co-Director

and

Mr. James E. Dudgeon
Research Associate

Prepared for
George C. Marshall Space Flight Center
Huntsville, Alabama

ACKNOWLEDGEMENT

This report has been prepared for the Instrumentation Branch, Astrionics Division, George C. Marshall Space Flight Center, Huntsville, Alabama, under Contract NAS8-5412.

The authors wish to express their appreciation to Messrs. J. W. Harper, Paul Swindall, and Donald Stone of the Astrionics Division for their interest and their most valuable advice. The authors wish also to express their appreciation to Professor O. P. McDuff and particularly to Dr. T. D. Shockley, who were formerly associated with the project as Co-Directors. Appreciation is also expressed for the administrative assistance of Professor L. A. Woodman, Director, Bureau of Engineering Research.

TABLE OF CONTENTS

LIST OF ILLUSTRATIONS

PREFACE

This is the final report on studies performed under Contract NAS8-5412 with George C. Marshall Space Flight Center. This contract was initiated June 5, 1963, and expires September 15, 1966.

The project had two aims. One was the study of antenna voltage breakdown at high altitudes during the radiation of multiple signals from one antenna system. This phase of the work was concluded and the results discussed in an Interim Report dated June, 1964. Dr. Harold Mott was solely responsible for this work phase.

The subject of the technical portion of this Final Report is the remaining work phase which was concerned with the significant differences between the radiation pattern of an antenna in an ideal environment and the same antenna when installed on a vehicle having numerous structural and aerodynamic features inappropriate for the radiation of an optimum pattern. The following individuals contributed significantly to this area of study:

Dr. Harold Mott, Project Director, June 5, 1963-September 15, 1966.

Professor O. P. McDuff, Co-Director, June 5, 1963-October 5, 1963

Dr. T. D. Shockley, Co-Director, February 1, 1964-August 31, 1964

Dr. J. C. Dowdle, Co-Director, September 15, 1964-September 15, 1966

Mr. J. R. Burnett, Research Associate, June 5, 1963-September 15, 1964

Mr. J. E. Dudgeon, Research Associate, September 1, 1964- September 15, 1966.

In addition to monthly progress reports, two major reports were submitted on Contract NAS8-5412, entitled

"Multifrequency Antenna Breakdown," by Dr. Harold Mott, Interim Report, June 1964,

and

"Location of Pattern-Disturbing Structures in the Near-Field of an Antenna," by H. Mott, T. D. Shockley, and J. R. Burnett, Technical Report No. 1, September, 1964.

The following papers dealing with various aspects of the project were published in the open literature:

H. Mott, "Multifrequency Breakdown of Antennas in Air," Proc. IEEE, vol. 52, no. 12, pp. 1752-1753; December, 1964.

H. Mott, T. D. Shockley, and J. R. Burnett, "Location of Pattern-Disturbing Structures in the Near-Field of an Antenna," IEEE Trans. on Antennas and Propagation, vol. AP-13, no. 5, pp. 832-33; September, 1965.

H. Mott, J. C. Dowdle, and J. E. Dudgeon, "The Reproducibility of a Source from the Pattern Amplitude," IEEE Trans. on Antennas and Propagation, vol. AP-14, no. 3, pp. 396-397; May, 1966.

H. Mott, J. C. Dowdle, and J. E. Dudgeon, "The Reproducibility of a Planar Distribution from the Pattern Amplitude," accepted for publication by the Proceedings of the IEEE (Correspondence).

CHAPTER I

INTRODUCTION

One of the problems associated with satellite and space vehicle communications systems is the pattern-distorting effect of fins, structural panels, and obstructions located in the vicinity of the radiating and receiving antennas mounted on the vehicles. This particular problem has become important because the basic configuration of the various vehicle stages is usually determined of necessity by the aerodynamic and structural factors involved. Thus the actual radiation patterns may differ greatly from the desired or the ideal pattern determined prior to antenna installation on the vehicle.

Model or full-scale experimental techniques are often employed to ascertain the distortion produced by pattern-disturbing structures located in the proximity of the mounted antennas. It is not unusual to utilize cut- and -try methods in conjunction with pattern measurements to produce realistic patterns which at best may only approximate the desired pattern. Such procedures and their success are based to a large extent on the backlog of knowledge and experience of the engineers performing the tests. One problem, difficult even for experience to overcome, is that structures may be optically significant but not electrically important, and vice versa.

It therefore seemed highly desirable to develop a straightforward technique for determining the effects produced by structural features or obstacles located in the antenna vicinity. The function of greatest importance to this study was the radiation pattern. It is also a commonly-measured function. It was therefore decided to study the radiation pattern and try to relate certain features of the pattern to the

structural features of the vehicle. With a successful application of such a method structural features having significant effect on the radiation pattern may be identified and altered if necessary.

A somewhat similar problem has been studied by other investigators. This is the problem of pattern synthesis: given a radiation pattern amplitude, to find a source distribution (with certain constraints) which will satisfactorily reproduce the pattern. One might assume that if a synthesis procedure is carried out for some measured radiation pattern the current or voltage distribution along the source thus found would correspond to the actual distribution which generated the measured pattern. This assumption may rigorously be proved true for some geometries, and this is done in the report, but is does not seem amenable to a general proof. It must also be pointed out that some dissimilarities exist between the aims of the normal pattern synthesis and our purpose of obstacle location. For example, in pattern synthesis one is normally content to reproduce a given pattern amplitude, but in general this can be done by an infinite number of source distribution functions depending on the phase assigned to the radiation pattern and on the pattern amplitude assigned outside the range of interest of the pattern variable. Thus if one uses normal synthesis procedures to find a source which produces a measured pattern amplitude there is in general no guarantee that this even approximates the source distribution which generated the pattern.

In addition, in synthesis one wishes to reproduce a given pattern with some margin of error, while in the obstacle location procedure one desires to find true source currents within some error margin. It is not easy to relate pattern error to current error.

In spite of these differences, however, pattern synthesis procedures form a powerful tool to accomplish the aim of obstacle location in the vicinity of an antenna. We have drawn freely on the published literature of pattern synthesis, and in addition we have developed synthesis techniques appropriate to our needs. Because of the complexity of practical problems in this area many of our procedures have been programmed in FORTRAN for a digital computer.

In the first section of the report we discuss in general the problem of obtaining the source current (or voltage) distribution on a structure from a knowledge of the electromagnetic fields produced by the source and show that for certain types of structures this is feasible. Two of the most powerful methods for carrying out this process, the Fourier series and Fourier transform methods, are also discussed, because they are important in showing that the source distribution can be obtained from the fields. In the next two chapters other synthesis methods are presented, and in a still later section the results of applying the various methods to measured patterns are given.

CHAPTER II

EXISTENCE OF SOLUTIONS

The General Case

A basic question to the obstacle location procedures discussed in this report is whether a source current distribution can be determined uniquely from a knowledge of the fields over some region of space. We may use in an illustrative manner the vector potential for unbounded space

$$\bar{A}(\bar{r}) = \frac{1}{4\pi}\int\int\int \frac{\bar{J}(\bar{r}')\varepsilon^{-jk|\bar{r}-\bar{r}'|}}{|\bar{r}-\bar{r}'|}\,dv' \qquad (2\text{-}1)$$

where $\bar{r}$ is a vector giving the location of the field point at which the potential is found, $\bar{J}(\bar{r}')$ is the electric current density at the source point $\bar{r}'$, and the integration is carried out over the whole current distribution. For a current distribution over a surface, the volume integral may be replaced by a surface integral if the volume current density is replaced by a surface current density. In the example we then ask if, from a knowledge of $\bar{A}(\bar{r})$ over some range, we can solve Eq. (2-1) for $\bar{J}(\bar{r}')$. Note that we can set up similar integrals for the fields, rather than the potential used in the example, and then our problem would be to find the source currents from a knowledge of the electric or magnetic field or both.

It appears that no answer can be given in general to the question of whether or not Eq. (2-1) can be solved for $\bar{J}$ if $\bar{A}$ is known over some range unless $\bar{A}$ is known at the source itself, in which case we can find the source. Again we use $\bar{A}$ as an example. It is in fact the fields which should be known at the source if we are to determine the source distribution. If for example the source is known to consist of an electric sur-

face current density $\bar{J}_s$ on the surface of a conductor the magnetic field at the conductor surface is related to the current by

$$\bar{J}_s = \bar{n} \times \bar{H} \tag{2-2}$$

where $\bar{n}$ is the unit normal drawn outward from the conductor surface. Therefore, a knowledge of $\bar{H}$ at the surface enables us to find the surface current density. Love's equivalence principle[1] points out that in a source-free region enclosed by a surface the effect of all sources external to the region can be taken into account by equivalent sources on the surface, of value

$$\bar{J}_s = \bar{n} \times \bar{H} \tag{2-3}$$

$$\bar{M}_s = \bar{E} \times \bar{n} \tag{2-4}$$

where $\bar{J}_s$ and $\bar{M}_s$ are surface electric and magnetic currents. Over a surface which covers an aperture in a conducting plate if we know the electric field we can determine a magnetic current by the relation (2-4) and treat this fictitious magnetic current as a real current in determining the fields produced by the structure. It is therefore clear that if we know the fields at the surface of an electromagnetic structure we can determine the currents on the structure. If the "surface" is adjacent to a metallic conductor the currents thus found are true electric currents. If it is some surface chosen in part not adjacent to a conductor the "currents" found are fictitious, or equivalent, currents and we may work with electric or magnetic currents or both[1]. It is not possible, from a field measurement alone, to distinguish between an electric current and a magnetic current[2], but this is not an important problem in our aim of obstacle location. We are searching for points on the surface of a missile with a high field concentration, whether this be an $\bar{H}$ field caused by electric currents or an $\bar{E}$ field (for example at an aperture) describable

in terms of magnetic currents.

If we restrict $\bar{r}$ and $\bar{r}'$ of Eq. (2-1) in certain ways the resulting equation may be solvable for $\bar{J}(\bar{r}')$. If for example $\bar{A}(\bar{r})$is known over a spherical surface of very large radius compared to wavelength and source extent (the radiation field) and if the source is known to lie on a surface of known geometry, such as the x'z' plane, Eq. (2-1) simplifies to

$$\bar{A}(\bar{r}) = \frac{\varepsilon^{-jkr}}{4\pi r} \int \bar{J}_s(\bar{r}') \, \varepsilon^{jk(x'\sin\theta\cos\phi + z'\cos\theta)} \, dx'dz' \qquad (2\text{-}5)$$

which in theory is soluable for $\bar{J}_s(\bar{r}')$. This is of course not the only specialization of Eq. (2-1) which can be solved. Other specifications of the region in which $\bar{A}(\bar{r})$ is known and the source geometry may lead to equations from which the source distribution may be determined.

In the remainder of this report we will concern ourselves with the radiation fields only, since these are the most commonly measured antenna fields. This in essence involves a specialization of Eq. (2-1). In addition we will specify source geometries, leading to further specialization of Eq. (2-1). Methods of solution of the resulting equations are different for the various geometries, and a large part of the work reported herein is concerned with a search for solutions of the specialized integral equations derived from Eq. (2-1).

Rather than dealing with the vector potential the integral equations considered will involve directly the electric field and the electric current distribution, but the principle is the same for any field or potential.

Fourier Series Solution

In the first problem we discuss to show the existence of a solution

for the source currents from the known field pattern we express the field as a summation rather than an integral. The radiation pattern of a source in some arbitrarily chosen plane, Fig. 2-1, may be transformed to $E(\psi)$ by

$$\psi = \beta d \cos \phi + \delta \tag{2-6}$$

and expanded in a Fourier series as

$$E(\psi) = \sum_{-\infty}^{\infty} I_k \varepsilon^{jk\psi} \tag{2-7}$$

where

$$I_k = \frac{1}{2\pi} \int_{-\pi}^{\pi} E(\psi) \varepsilon^{-jk\psi} \, d\psi \tag{2-8}$$

At this point (2-7) is merely a formal expansion of the pattern function in a series. Now it is easy to show that the radiation pattern of an infinite array of isotropically radiating elements on a straight line, Fig. 2-1, is also given by (2-7), where the I_k are the relative strengths of the individual sources. It therefore follows that any radiation pattern which may be expanded in a Fourier series can be reproduced as closely as desired by isotropic elements in a line array. We find the complex element strengths of this pattern-synthesizing line array from (2-8). If the array is truly to reproduce the given pattern we must interpret the terms of the formal transformation (2-6) as: $\beta = 2\pi/\lambda$, d is the spacing between adjacent sources, ϕ is the angle between a line along the array axis and a line drawn to the field point, and δ is an arbitrary change in phase between adjacent sources.

At this point additional comments about our procedure are in order. First, the field pattern function which we expand is a scalar which implies that we have chosen one component of the electric field, normally in the pattern plane or perpendicular to it, but any polarization can in fact be

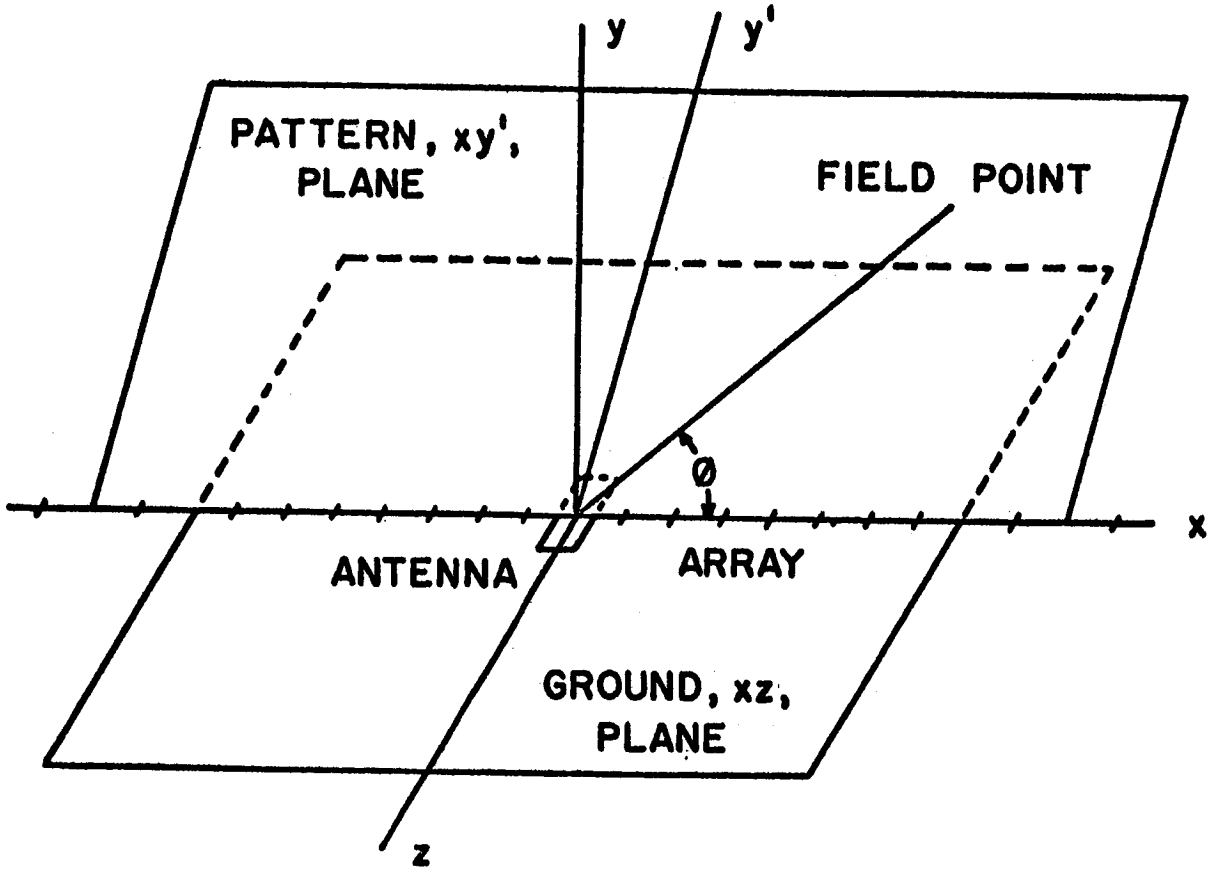

Fig. 2-1. Antenna and Pattern - Synthesizing Array

chosen. Second, we assume that our elemental radiators are isotropic. In the normal synthesis procedure it is commonly assumed that the directional pattern of all radiating elements is the same. Then this pattern function may be removed from the integral or summation which gives the total field pattern in terms of the element currents. For example with nonisotropic radiators (2-7) would become

$$E(\psi) = G(\psi) \sum_{-\infty}^{\infty} I_k \, \varepsilon^{jk\psi} \tag{2-9}$$

where $G(\psi)$ is the pattern function for each radiator, and one would then find an array from Eq. (2-8) to synthesize the pattern $E(\psi)/G(\psi)$. In our obstacle location procedure, in the absence of information about element directional characteristics, we have no other course but to choose arbitrarily some characteristic. For reasons of convenience we choose isotropic radiators. Justification will appear later when it is shown that we can locate obstacles from experimental patterns.

Another important comment is that for the pattern of the general antenna the currents in the synthesizing array, given by Eq. (2-8), do not uniquely reproduce the source which generated the known pattern. A simple example will show this. The pattern of a continuous line source may be measured and analyzed into its Fourier components by (2-8), but (2-8) implies isotropic elements with discrete and constant spacing, and this is obviously not the original source.

However, if the original source producing the measured pattern consists of isotropic elements with a discrete (but not necessarily equal) spacing commensurate with the spacing d assumed for the synthesizing array the array currents found by Eq. (2-8) from the measured pattern will uniquely reproduce the original source. One might expect that this con-

dition will be approximated for many problems of obstacle location, such as large surfaces having an antenna of small extent and obstacles on the surface which are concentrated in regions not large compared to a wavelength.

Fourier Series using Pattern Amplitude

It is customary in many antenna pattern installations to measure only the field amplitude, not the phase. In general this does not give sufficient information to allow a determination of the source. One exception to this is if a symmetry exists in the source such that each element has its complex conjugate element an equal distance from the center of the source and on the opposite side of the center. Then the pattern will have a constant phase, and synthesis will give the correct source.

Another, and most important, problem for which amplitude information alone is sufficient to determine (with one ambiguity) the source distribution is that in which the main antenna dominates the radiation pattern and the obstacles to be located add small perturbations to the main element pattern.

Consider as an example an antenna on a ground plane with n obstacles lying in a straight line on the plane. Assume that the antenna aperture and the obstacles are small so that over a substantial portion of the pattern they act as isotropic radiators and have a constant phase at a constant distance from their respective phase centers. Let the known information about this configuration be the amplitude pattern in a plane passing through the antenna center and the obstacles. This configuration describes approximately the structural arrangement of many practical antennas. The obstacles may in practice extend outside the pattern plane, one example being the edge of a finite ground plane with the antenna located on it.

The field at a constant distance from the phase center of the antenna is

$$E = \sum_{k=0}^{n} A_k \varepsilon^{j(\beta d_k \cos \phi + \theta_k)} \tag{2-10}$$

where d_k is the signed distance from antenna to obstacle, A_k is the magnitude of the induced current in the obstacle, A_o is the antenna current, and θ_k is the relative phase of the kth current.

Set

$$\psi_k = \beta d_k \cos \phi + \theta_k$$
$$d_o = 0 \tag{2-11}$$

and find

$$|E|^2 = \left[\sum_{k=0}^{n} A_k \cos \psi_k\right]^2 + \left[\sum_{k=0}^{n} A_k \sin \psi_k\right]^2$$

$$= \sum_{k=0}^{n} A_k^2 + \sum_{k=0}^{n} \sum_{\substack{p=0 \\ k \neq p}}^{n} A_k A_p \cos (\psi_k - \psi_p) \tag{2-12}$$

Assuming that A_o^2 is much greater than any other term of Eq. (2-12), then

$$|E| = A_o \left[1 + \frac{1}{2A_o^2} \sum_{k=1}^{n} A_k^2 + \frac{1}{4A_o^2} \sum_{k=0}^{n} \sum_{\substack{p=0 \\ k \neq p}}^{n} A_k A_p \left(\varepsilon^{j(\psi_k - \psi_p)} + \varepsilon^{-j(\psi_k - \psi_p)}\right)\right] \tag{2-13}$$

Now

$$\psi_k - \psi_p = \beta \cos \phi \, (d_k - d_p) + (\theta_k - \theta_p) \tag{2-14}$$

and it is obvious that an array synthesized from the magnitude pattern above will yield (if the array spacing is commensurate with $d_k - d_p$) array currents in the center element and in the elements at

$$\pm (d_k - d_p), \quad k, p = 0, 1, 2, \ldots n$$
$$k \neq p$$

With k or p taken equal to zero the distance to an array current gives the distance between antenna and obstacle.

If in the preceding term we take p = 0 and then $d_o = 0$ we find in the array which we determine that currents exist at $\pm d_k$. We know that the original source, from Eq. (2-10), had an element only at $+d_k$. Thus, by knowing only the pattern amplitude, we have introduced a 180° ambiguity into our solution. Normally, this should pose no serious difficulty to the obstacle location problem since a visual inspection of the antenna and its surroundings will probably resolve this ambiguity.

In addition to yielding element currents at the locations of the obstacles the synthesis method also indicates the spurious presence of obstacles at distances equal to the differences $(d_k - d_p)$; $k, p \neq 0$.
With the assumption that

$$\sum_{k=1}^{n} A_k^2 \ll A_o^2 \tag{2-15}$$

then

$$A_k A_p \ll A_o A_k \qquad k, p \neq 0 \tag{2-16}$$

and the spurious currents will be much smaller than the true currents. It is still advisable to apply this technique with care, however.

Eq. (2-12) indicates that if the synthesis is carried out for the power pattern $|E|^2$ rather than $|E|$ the requirement that obstacle fields be small compared to the antenna field, used in the square root approximation, is not necessary. However, if this requirement is not met the spurious array currents may be troublesome.

The obstacle locations will be more clearly defined if a difference array is formulated. To form the difference array the undistorted pattern of the antenna is synthesized using an array of the form of Eq. (2-7). The distorted pattern is also synthesized with an identical array. Subtracting the array currents, element by element, gives the difference array. Use of the undistorted pattern array as a subtrahend is not necessary; the array for the antenna and some of the surrounding obstacles may be used. The pattern for an antenna on an infinite ground plane may be subtracted from that for the same antenna on a finite plane; or the finite ground plane pattern from that for the finite ground plane with obstacles, etc. The advantage in the use of such a difference array may be observed in the following example:

If from Eq. (2-13) we subtract the pattern for the antenna and r elements (numbered without loss of generality 1, 2, . . ., r) we get

$$|E| - |E_{1,r}| = A_o + \frac{1}{2A_o}\sum_{k=1}^{n} A_k^2 + \frac{1}{4A_o}\sum_{k=0}^{n}\sum_{\substack{p=0 \\ k\neq p}}^{n} A_k A_p\left(\varepsilon^{j(\psi_k-\psi_p)} + \varepsilon^{-j(\psi_k-\psi_p)}\right)$$

$$-A_o - \frac{1}{2A_o}\sum_{k=1}^{r} A_k^2 - \frac{1}{4A_o}\sum_{k=0}^{r}\sum_{\substack{p=0 \\ k\neq p}}^{r} A_k A_p\left(\varepsilon^{j(\psi_k-\psi_p)} + \varepsilon^{-j(\psi_k-\psi_p)}\right)$$

$$= \frac{1}{2A_o}\sum_{k=r+1}^{n} A_k^2 - \frac{1}{4A_o}\sum_{k=r+1}^{n}\sum_{\substack{p=r+1 \\ k\neq p}}^{n} A_k A_p\left(\varepsilon^{j(\psi_k-\psi_p)} + \varepsilon^{-j(\psi_k-\psi_p)}\right) \quad (2\text{-}17)$$

Synthesis of this pattern gives the same types of array current distributions as for $|E|$ alone. However, the spurious responses are reduced in

in number from the value $\sum_{k=1}^{n-1} (n-k)$ to $\sum_{k=r+1}^{n-1} (n-k)$.

Because of the linearity of the synthesis process the amplitude patterns may be subtracted before synthesis or the resulting array currents for $|E|$ and $|E_{1,r}|$ subtracted after synthesis with the same results.

In carrying out the described procedures the array coefficients are found by integration in the normal Fourier series process. The patterns of antenna and each obstacle, at first assumed isotropic and equiphase, need to meet the required conditions that they be isotropic and equiphase only over a sufficient portion of the pattern plane to give a significant contribution to the integrals. For this reason many practical antenna configurations can be studied by this process which do not even meet the condition that the "obstacles" lie completely on or near the array axis. As an example, the edges of a finite ground plane with a slot antenna at its center have been located.

The practical effect of a non-isotropic object or of an object lying close to but not on the line of the array or of an object lying between two assumed array elements is that the array current distribution is diffuse. Instead of a large current in one element and small currents in adjacent ones, the adjacent elements may also carry appreciable currents.

It is most convenient in Fig 2-1 to take the pattern plane as the xy plane, but it may be taken instead as the arbitrary xy' plane. Discontinuities lying far from the array line of Fig.2-1 may not affect the array currents appreciably. In order to locate such discontinuities several patterns, involving rotation about the y axis, may be necessary. Synthesis is carried out for each pattern, and any obstacle will then lie on or near some array axis and will affect the array currents significantly.

The possibility of using pattern magnitude only is a fortunate one in that pattern phase is often not measured. It is particularly fortunate that in some cases pattern amplitudes may be subtracted, as in comparing the pattern of the antenna in its real environment to that in the ideal environment, while retaining information about the physical configuration of the environment. It was seen earlier, however, that use of magnitudes only leads to the spurious responses at the differences of positions of two or more obstacles and to the 180° ambiguity in obstacle location. As shown previously, no such ambiguity exists if the phase of the radiation pattern is known.

The application of this method to experimentally-obtained patterns will be discussed in a later section.

Fourier Transform Solution

The radiation field pattern of a continuous line distribution of isotropic elements in a plane containing the line source may be written as

$$E(u) = \int_{-\infty}^{\infty} I(x)\, \varepsilon^{jux} dx \qquad (2\text{-}18)$$

where

$$u = \frac{2\pi}{\lambda} \cos \theta \qquad (2\text{-}19)$$

with θ the angle measured from the line source.

Now Eq. (2-18) is recognizable as the Fourier transform of the current distribution. The unique inverse is

$$I(x) = \frac{1}{2\pi} \int_{-\infty}^{\infty} E(u)\, \varepsilon^{-jux} du \qquad (2\text{-}20)$$

It therefore follows that if we have the radiation pattern E(u) for a line source we can uniquely determine the line source itself. This is one of

the more important proofs that Eq. (2-1), and similar equations for the fields, can be solved to find the source currents if a certain locus for the field points and certain source geometry are assumed.

As was mentioned earlier we often do not know the phase of E(u) in Eq. (2-20). We wish to consider the pattern amplitude only and determine what information about the source can be obtained from the amplitude alone. In a manner similar to that used for the preceding discussion of the Fourier series representation of the source, let the actual source distribution consist of a region exerting a dominant influence on the pattern and smaller perturbing terms outside this dominant region.

The correct current distribution is I(x). We wish to determine, in terms of the correct current, what would be obtained from (2-20) if the pattern magnitude only were used.

We assume that sources in the range $-a < x < a$ contribute most to the field and define

$$F(u) = \int_{-a}^{a} I(x)\, \varepsilon^{jux} dx \tag{2-21}$$

With this assumption and breaking the integral (2-18) into the sum of three integrals we can write

$$|E|^2 = EE^* = \left[\int_{-\infty}^{\infty} I(x)\, \varepsilon^{jux} dx\right]\left[\int_{-\infty}^{\infty} I^*(x)\, \varepsilon^{-jux} dx\right] \tag{2-22}$$

approximately as

$$|E|^2 = FF^* + \int_{-\infty}^{-a} \left[F\, I^*\, \varepsilon^{-jux} + F^*\, I\, \varepsilon^{jux}\right] dx$$

$$+ \int_{a}^{\infty} \left[F\, I^*\, \varepsilon^{-jux} + F^*\, I\, \varepsilon^{jux}\right] dx \tag{2-23}$$

Continuing with the assumption that the first term of (2-23) is much greater

than the remaining terms we find

$$|E| = |F| + \frac{1}{2|F|}\int_{-\infty}^{-a}\left[F\,I^{*}\,\varepsilon^{-jux} + F^{*}\,I\,\varepsilon^{jux}\right]dx$$

$$+ \frac{1}{2|F|}\int_{a}^{\infty}\left[F\,I^{*}\,\varepsilon^{-jux} + F^{*}\,I\,\varepsilon^{jux}\right]dx \qquad (2\text{-}24)$$

Now it is easily shown that

$$|F| = \frac{1}{2|F|}\int_{-a}^{a}\left[F\,I^{*}\,\varepsilon^{-jux} + F^{*}\,I\,\varepsilon^{jux}\right]dx \qquad (2\text{-}25)$$

Therefore

$$|E| = \frac{1}{2|F|}\int_{-\infty}^{\infty}\left[F\,I^{*}\,\varepsilon^{-jux} + F^{*}\,I\,\varepsilon^{jux}\right]dx \qquad (2\text{-}26)$$

Using this field amplitude in our synthesis procedure we obtain

$$e(x) = \mathcal{F}^{-1}\left\{|E(u)|\right\} = \frac{1}{2}\left[\mathcal{F}^{-1}\left\{\frac{F(u)}{|F(u)|}\right\} * I^{*}(-x) + \mathcal{F}^{-1}\left\{\frac{F^{*}(u)}{|F(u)|}\right\} * I(x)\right] \qquad (2\text{-}27)$$

This form simplifies greatly if we assume that in the range $-a < x < a$

$$I(x) = I^{*}(-x) \qquad -a < x < a \qquad (2\text{-}28)$$

Then $F(u)$ is real and

$$|E| = \frac{1}{2}\int_{-\infty}^{\infty}\left[I\,\varepsilon^{jux} + I^{*}\,\varepsilon^{-jux}\right]dx \qquad (2\text{-}29)$$

and the inverse transform of $|E|$ is

$$e(x) = \frac{1}{2}\left[I(x) + I^{*}(-x)\right] \qquad (2\text{-}30)$$

With these restricted assumptions it is apparent that our determination of the source distribution is not necessarily unique, but does contain useful information. Other information, such as a visual inspection of the

source distribution, can be used, however, to supplement (2-30). Thus if we find the inverse transform of $|E|$

$$e(x) = \mathcal{F}^{-1}\left\{|E(u)|\right\} \tag{2-31}$$

and observe a high current in the neighborhood of, say, $x = -c$ we could be sure of an obstacle located near $x = \pm c$. Visual inspection would then tell us whether it was at $+c$ or $-c$.

The following example substantiates this point in that a field magnitude pattern is used to give a known source distribution, plus spurious responses. Consider isotropic point sources on a line

$$I(x) = \sum_{k=o}^{n} I_k \, \delta(x - d_k) \tag{2-32}$$

where d_k is the signed distance to the source and $d_o = 0$. Then

$$E = \int_{-\infty}^{\infty} I(x)\, \varepsilon^{jux} dx = \sum_{k=o}^{n} I_k \, \varepsilon^{jud_k} = I_o + \sum_{k=1}^{n} I_k \, \varepsilon^{jud_k} \tag{2-33}$$

$$|E|^2 = EE^* = I_o^{\,2} + I_o \sum_{k=1}^{n} \left[I_k \, \varepsilon^{jud_k} + I_k^{\,*} \, \varepsilon^{-jud_k}\right]$$

$$+ \sum_{k=1}^{n} \sum_{p=1}^{n} I_k \, I_p^{\,*} \, \varepsilon^{ju(d_k - d_p)} \tag{2-34}$$

We let I_o be the dominant term corresponding to the distribution in the range 2a which produced the term F(u) of Eq. (2-21). Then we neglect the last term of (2-34) and treat the second term as very small compared to the first, obtaining

$$|E| \approx I_o + \frac{1}{2} \sum_{k=1}^{n} \left[I_k \, \varepsilon^{jud_k} + I_k^{\,*} \, \varepsilon^{-jud_k}\right] \tag{2-35}$$

yielding the inverse transform

$$e(x) = \mathcal{F}^{-1}\left\{|E|\right\} = I_o\delta(x) + \frac{1}{2}\sum_{k=1}^{n}\left[I_k\delta(x - d_k) + I_k^{*}\,\delta(x + d_k)\right] \qquad (2\text{-}36)$$

It is clear from (2-36) that a source at d_k effective in producing the field E appears in the source function determined from $|E|$ as sources at d_k and at $-d_k$. As stated, additional information needed to determine the sources uniquely may be obtained from a visual inspection of the aperture.

In a closer approximation we would add to (2-35) a correction term

$$\frac{1}{2I_o}\sum_{k=1}^{n}\sum_{p=1}^{n} I_k\, I_p^{*}\,\varepsilon^{ju(d_k - d_p)}$$

which would lead to a correction in the aperture distribution (2-36)

$$\frac{1}{2I_o}\sum_{k=1}^{n}\sum_{p=1}^{n} I_k\, I_p^{*}\,\delta\left[x - (d_k - d_p)\right]$$

This correction term predicts spurious sources of small amplitude at locations $\pm\,(d_k - d_p)$, as discussed previously for the Fourier series.

Fourier Transform with Truncated Pattern

Equation (2-20) shows that we can find a line source distribution uniquely from a knowledge of the radiation pattern in a plane containing the line source. Note, however, that it requires a knowledge of E(u) over an infinite range of the variable u. Now we know the pattern over a range of the angle θ from $\theta = 0$ to $\theta = \pi$ (the pattern in the range $\pi<\theta<2\pi$ merely repeats), and therefore, from (2-19)

$$u = \frac{2\pi}{\lambda}\cos\theta \qquad (2\text{-}19)$$

we know E(u) in the range

$$-\frac{2\pi}{\lambda} < u < \frac{2\pi}{\lambda}$$

Values of u outside this range, $|u| > \frac{2\pi}{\lambda}$, lead to imaginary values of θ in (2-19). We cannot measure the field in this so-called "invisible" range of the angle variable; nevertheless knowledge of it in this range is essential to the exact determination of the source distribution by the Fourier transform.

In this section we will develop the appropriate equations for finding the source distribution when the field pattern is known only over the visible range $-2\pi/\lambda < u < 2\pi/\lambda$. We will also show that in many cases of interest a good approximation to the correct source can be obtained from the visible pattern.

We define the function

$$S(z) = 1 \qquad -1/2 < z < 1/2$$
$$= 0 \qquad |z| > 1/2 \tag{2-37}$$

Let us also assume that the actual source distribution lies between the limits $\pm b$ as shown in Fig. 2 with the region limited by $\pm a$ giving a dominant contribution to the field pattern.

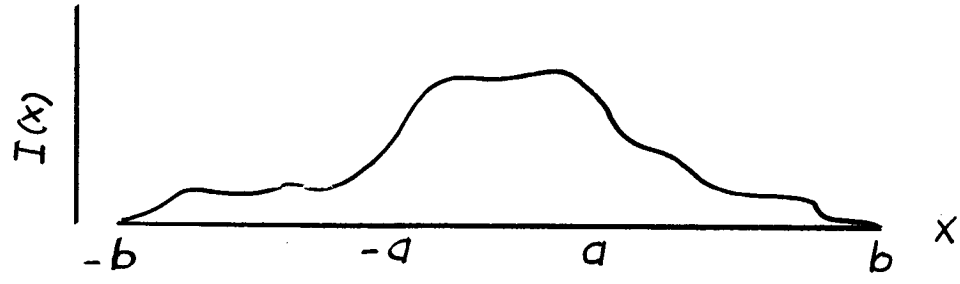

Fig. 2-2 Line Source Distribution

Then we can write in general

$$E(u) = \int_{-\infty}^{\infty} I(x)\, S\left(\frac{x}{2b}\right) \varepsilon^{jux} dx \tag{2-38}$$

and we know that

$$\mathcal{F}^{-1}\left\{E(u)\right\} = I(x)\, S\left(\frac{x}{2b}\right) \tag{2-39}$$

However, since E(u) is known only over the visible range, we must transform E(u) S $(\frac{u}{4\pi/\lambda})$. We then wish to know how the current distribution we thus find is related to the actual current distribution.

The current distribution we find from the pattern truncated to the visible range is

$$i(x) = \mathcal{F}^{-1}\left\{E(u)\ S(\frac{\lambda u}{4\pi})\right\} \tag{2-40}$$

By the convolution theorem

$$i(x) = \mathcal{F}^{-1}\left\{E(u)\right\} * \mathcal{F}^{-1}\left\{S(\frac{\lambda u}{4\pi})\right\} \tag{2-41}$$

But

$$\mathcal{F}^{-1}\left\{E(u)\right\} = I(x)\ S(\frac{x}{2b}) \tag{2-39}$$

$$\text{and } \mathcal{F}^{-1}\ S(\frac{\lambda u}{4\pi}) = \frac{1}{2\pi}\int_{-\infty}^{\infty} S(\frac{\lambda u}{4\pi})\ \varepsilon^{-jux} du = \frac{1}{\pi x}\sin\frac{2\pi x}{\lambda} \tag{2-42}$$

Therefore

$$i(x) = I(x)\ S(\frac{x}{2b}) * \frac{1}{\pi x}\sin\frac{2\pi x}{\lambda}$$

$$= \frac{2}{\lambda}\int_{-\infty}^{\infty} I(v)\ S(\frac{v}{2b})\ \frac{\sin\frac{2\pi(x-v)}{\lambda}}{\frac{2\pi(x-v)}{\lambda}}\ dv$$

$$= \frac{2}{\lambda}\int_{-b}^{b} I(v)\ \frac{\sin\frac{2\pi(x-v)}{\lambda}}{\frac{2\pi(x-v)}{\lambda}}\ dv \tag{2-43}$$

The function i(x) is known; it is the inverse transform of the field pattern over the visible range. Then (2-43) is a homogenous integral equation with unknown function I(v). The nucleus

$$K(x,v) = \frac{\sin\frac{2\pi(x-v)}{\lambda}}{\frac{2\pi(x-v)}{\lambda}} \tag{2-44}$$

is symmetric in that K(x,v) = K(v,x). Therefore by Schmidt's theorem the function

$$D(\alpha) = D(\tfrac{2}{\lambda}) = 1 - \alpha \int_{-b}^{b} K(y_1,y_1)dy_1$$

$$+ \frac{\alpha^2}{2!} \int_{-b}^{b}\int_{-b}^{b} \begin{vmatrix} K(y_1,y_1) & K(y_1,y_2) \\ K(y_2,y_1) & K(y_2,y_2) \end{vmatrix} dy_1 dy_2 \qquad (2\text{-}45)$$

has at least one root. It can therefore be shown that for at lease one value of b, a solution of (2-43) for I(x) can be obtained.[3]

Now let us consider the more difficult problem in which the field magnitude only is known over the visible range $-2\pi/\lambda < u < 2\pi/\lambda$. If we make the assumption that currents in the range $\pm a$ make a dominant contribution to the pattern and if we further assume that in this range

$$I(x) = I^*(-x) \quad -a < x < a \qquad (2\text{-}28)$$

we have found that

$$|E(u)| = \frac{1}{2} \int_{-\infty}^{\infty} \left[I(x)\, \varepsilon^{jux} + I^*(x)\, \varepsilon^{-jux} \right] dx \qquad (2\text{-}29)$$

If the current distribution has the finite length 2b, then

$$|E(u)| = \int_{-\infty}^{\infty} S(\tfrac{x}{2b}) \left[I(x)\, \varepsilon^{jux} + I^*(x)\, \varepsilon^{-jux} \right] dx \qquad (2\text{-}46)$$

The pattern magnitude is again truncated to the visible range by the factor $S(\frac{\lambda u}{4\pi})$ so that

$$i(x) = \mathcal{F}^{-1} \left\{ |E(u)| \quad S(\tfrac{\lambda u}{4\pi}) \right\}$$

$$= \frac{1}{2} S(\tfrac{x}{2b}) \left[I(x) + I^*(-x) \right] * \frac{1}{\pi x} \sin \frac{2\pi x}{\lambda} \qquad (2\text{-}47)$$

where we use

$$S(z) = S(-z) \qquad (2\text{-}48)$$

Continuing with the use of the convolution theorem we get from (2-47)

$$i(x) = \frac{1}{\lambda} \int_{-b}^{b} \left[I(v) + I^*(-v) \right] \frac{\sin \frac{2\pi(x-v)}{\lambda}}{\frac{2\pi(x-v)}{\lambda}} dv \qquad (2\text{-}49)$$

This form is similar to Eq. (2-43), and it therefore follows that, for at least one value of b, a solution for $I(v) + I^*(-v)$ can be obtained.

Rather than go into detail on the solution of (2-49) let us examine the problem further to see what the effects of the pattern truncation are. One would intuitively expect that the source current reproduction would be poorest in the region of rapid rates of change of the actual source current. Such fast rates of change occur in the vicinity of the obstacles and particularly in the vicinity of the dominant source (the antenna).

Let us therefore assume as an example that $I(x)$ is constant in the range $-a < x < a$, that I_o is the real part of $I(x)$ in this range, and that $I(x) = 0$ for $|x| > a$. Then (2-49) becomes

$$i(x) = \frac{2}{\lambda} I_o \int_{-a}^{a} \frac{\sin \frac{2\pi(x-v)}{\lambda}}{\frac{2\pi(x-v)}{\lambda}} dv \qquad (2\text{-}50)$$

This can be transformed to the sum or difference of two sine integrals by the substitution

$$y = \frac{2\pi(x-v)}{\lambda} \qquad (2\text{-}51)$$

Then

$$i(x) = -\frac{I_o}{\pi} \int_{\frac{2\pi(x+a)}{\lambda}}^{\frac{2\pi(x-a)}{\lambda}} \frac{\sin y}{y} dy \qquad (2\text{-}52)$$

For $0 < x < a$

$$i(x) = \frac{I_o}{\pi} \left[\mathrm{Si}\left(\frac{2\pi(a+x)}{\lambda}\right) + \mathrm{Si}\left(\frac{2\pi(a-x)}{\lambda}\right) \right] \qquad (2\text{-}53)$$

For $x > a$

$$i(x) = \frac{I_o}{\pi} \left[\mathrm{Si}\left(\frac{2\pi(x+a)}{\lambda}\right) - \mathrm{Si}\left(\frac{2\pi(x-a)}{\lambda}\right) \right] \qquad (2\text{-}54)$$

Fig. 2-3 shows values of the current $i(x)$ for $I_o = \pi$ and various aperture width a/λ. As was expected, for the narrow aperture $a/\lambda = 0.1$, the known rectangular pulse for the actual current $I(x)$ is reproduced badly in

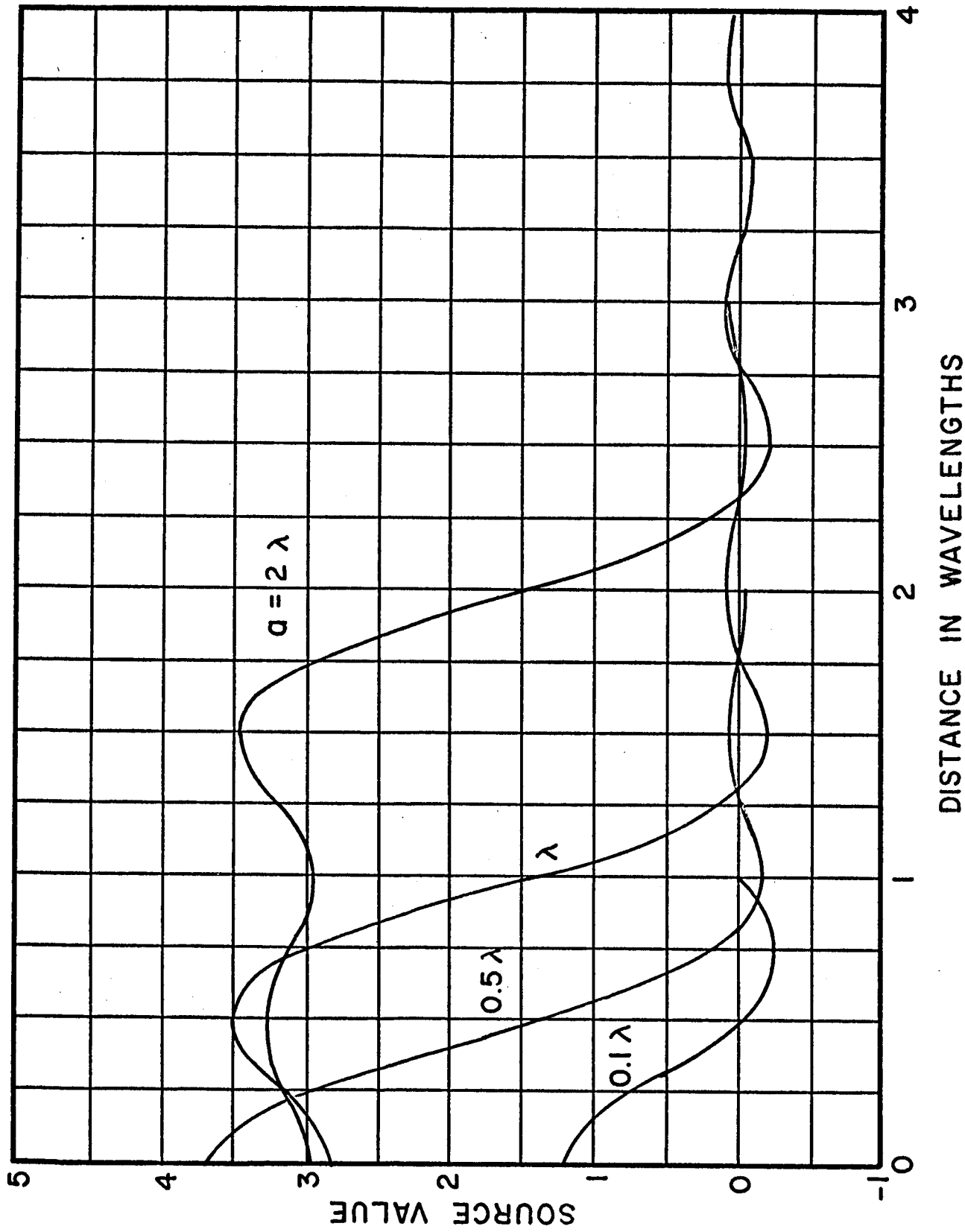

Fig. 2-3. Source Currents for Various Aperture Widths

shape. Nevertheless one would expect, from the manner in which the plotted function behaves, that at distances of two wavelengths from the edge of the aperture the effect of aperture current would be negligible. Thus one could expect to determine an obstacle location at a distance greater than two wavelengths from even a narrow aperture. As a/λ increases the reproduction of the rectangular pulse becomes better so that for $a/\lambda = 1$, for example, the current at one wavelength from the aperture edge is little perturbed.

As stated earlier it is felt that accurate reproduction of a sharp rectangular pulse is least likely to be successful because of the truncation of the radiation pattern to the visible range. Yet, Fig. 2-3 shows that this reproduction is quite good at distances of one or two wavelengths from the edge of the aperture. It is expected that the smoother current variations of a physical antenna with nearby obstacles will be more accurately reproduced than the rectangular current pulse we have just considered. For these reasons, then, we will generally not consider the effect of pattern truncation on our aperture distribution.

The Planar Distribution

In preceding sections we have discussed the reproducibility of a line source distribution from the radiation pattern in a plane containing the line source. This procedure is effective in locating objects lying on or near the line source. It was pointed out that to locate objects lying far from the assumed line source we could use several pattern planes, one at a time, rotated about a line passing through the central antenna element, Fig. 2-1, and perpendicular to the line defining each source. In Fig. 2-1, each pattern plane chosen would contain the y-axis. Any obstacle determined from a choice of the pattern plane would be on or near a line lying in that

plane.

In this section we will show that a knowledge of the radiation field in two variables, rather than the one angle variable of a pattern plane, leads directly to the current distribution on a plane, rather than on a line. This solution replaces the previous method of considering one pattern plane at a time.

Let us consider that the given source distribution lies on the yz plane, with the current in the region $-a < y < a$, $-b < z < b$ contributing a dominant value to the radiation field and currents outside this region contributing perturbing terms to the field.

For a planar source distribution the field is given by the two-dimensional Fourier transform

$$E(\psi,\gamma) = \int_{-\infty}^{\infty}\int_{\infty}^{\infty} I(y,z)\, \varepsilon^{jz\psi}\varepsilon^{jy\gamma} dydz \qquad (2\text{-}55)$$

where

$$\psi = \frac{2\pi}{\lambda} \cos\theta \qquad (2\text{-}56)$$

$$\gamma = \frac{2\pi}{\lambda} \sin\theta \sin\phi \qquad (2\text{-}57)$$

A right-handed xyz coordinate system is employed with θ the colatitude angle measured from the z axis and ϕ the azimuthal angle measured from the x axis.

Now the unique inverse of (2-55) is

$$I(y,z) = \frac{1}{(2\pi)^2} \int_{-\infty}^{\infty}\int_{-\infty}^{\infty} E(\psi,\gamma)\, \varepsilon^{-jz\psi}\varepsilon^{-jy\gamma} d\psi d\gamma \qquad (2\text{-}58)$$

It is then clear that if we know the electric field in amplitude and phase over the infinite range of its variables we can find the source distribution which generated the field. Thus obstacle location on a plane can be accomp-

lished.

As was pointed out previously we often know the field amplitude over the visible range of these variables. We have pointed out that the effect of pattern truncation to the visible range is not extremely serious for the line source, and we will not consider it for the planar source. We will consider, however, the effect of using the field magnitude only. We wish to know then, in terms of the correct current $I(y,z)$, what current distribution we will obtain if the field magnitude only is used in (2-58).

Let us define

$$F(\psi,\gamma) = \int_{y=-a}^{a} \int_{z=-b}^{b} I(y,z)\, \varepsilon^{jz\psi}\varepsilon^{jy\gamma} dydz \qquad (2\text{-}59)$$

and consider this the most important part of $E(\psi,\gamma)$.

We may then write

$$E(\psi,\gamma) = F(\psi,\gamma) + \int_{-\infty}^{-a}\int_{-\infty}^{-b} I(y,z)\, \varepsilon^{jz\psi}\varepsilon^{jy\gamma} dydz$$

$$+ \int_{-\infty}^{-a}\int_{-b}^{b} + \int_{-\infty}^{-a}\int_{b}^{\infty} + \int_{-a}^{a}\int_{-\infty}^{-b} + \int_{-a}^{a}\int_{b}^{\infty} + \int_{a}^{\infty}\int_{-\infty}^{-b} + \int_{a}^{\infty}\int_{-b}^{b} + \int_{a}^{\infty}\int_{b}^{\infty} \qquad (2\text{-}60)$$

where the seven integrands not written are the same as the one of the first integral.

Next we form the product $|E|^2 = EE^*$, retaining only terms involving F and F^* as being significant. A closer examination will show that some of the terms retained are of the same order as some of the terms neglected, but nonetheless the approximation is valid because all the important terms are retained in the product, and the unimportant terms are kept only because they lead to an obvious simplification of the final equation.

Approximately, then

$$EE^* = FF^* + \int_{-\infty}^{-a}\int_{-\infty}^{-b} (F\, I^*\, \varepsilon^{-jz\psi_\varepsilon - jy\gamma} + F^*\, I\, \varepsilon^{jz\psi_\varepsilon jy\gamma})\, dydz$$

$$+ \int_{-\infty}^{-a}\int_{-b}^{b} + \int_{-\infty}^{-a}\int_{b}^{\infty} + \int_{-a}^{a}\int_{-\infty}^{-b} + \int_{-a}^{a}\int_{b}^{\infty} + \int_{a}^{\infty}\int_{-\infty}^{-b} + \int_{a}^{\infty}\int_{-b}^{b} + \int_{a}^{\infty}\int_{b}^{\infty} \qquad (2\text{-}61)$$

where again all suppressed integrands are the same as the one given.

Continuing with our assumption about the relative importance of F we consider that all other terms in (2-61) are small compared to the first, and we may approximate the square root as

$$|E| = |F| + \frac{1}{2|F|}\left[\int_{-\infty}^{-a}\int_{\infty}^{-b} (F\, I^*\, \varepsilon^{-jz\psi_\varepsilon - jy\gamma} + F^*\, I\, \varepsilon^{jz\psi_\varepsilon jy\gamma})\, dydz\right.$$

$$\left. + \int_{-\infty}^{-a}\int_{-b}^{b} + \int_{-\infty}^{-a}\int_{b}^{\infty} + \int_{-a}^{a}\int_{-\infty}^{-b} + \int_{-a}^{a}\int_{b}^{\infty} + \int_{a}^{\infty}\int_{-\infty}^{-b} + \int_{a}^{\infty}\int_{-b}^{b} + \int_{a}^{\infty}\int_{b}^{\infty}\right] \qquad (2\text{-}62)$$

Now it is easy to show that

$$|F| = \frac{FF^*}{|F|} = \frac{1}{2|F|}\int_{-a}^{a}\int_{-b}^{b} (F\, I^*\, \varepsilon^{-jz\psi_\varepsilon - jy\gamma} + F^*\, I\, \varepsilon^{jz\psi_\varepsilon jy\gamma})\, dydz \qquad (2\text{-}63)$$

Combining (2-62) and (2-63) gives

$$|E| = \frac{1}{2|F|}\int_{-\infty}^{\infty}\int_{-\infty}^{\infty} (F\, I^*\, \varepsilon^{-jz\psi_\varepsilon - jy\gamma} + F^*\, I\, \varepsilon^{jz\psi_\varepsilon jy\gamma})\, dydz \qquad (2\text{-}64)$$

It follows that the source distribution determined from the inverse transform of the pattern amplitude is

$$i(y,z) = \mathcal{F}^{-1}\left\{|E(\psi,\gamma)|\right\} = \frac{1}{2}\left[\mathcal{F}^{-1}\left\{\frac{F(\psi,\gamma)}{|F|}\right\} * I^*(-y,-z)\right.$$

$$\left. + \mathcal{F}^{-1}\left\{\frac{F^*(\psi,\gamma)}{|F|}\right\} * I(y,z)\right] \qquad (2\text{-}65)$$

This form simplifies considerably if we assume that

$$I(y,z) = I^{*}(-y,-z) \quad \begin{matrix} -a < y < a \\ -b < z < b \end{matrix} \tag{2-66}$$

This is equivalent to assuming a symmetry in the dominant central element which is often met in practice. Then $F(\psi,\gamma)$ is real and (2-64) simplifies to

$$|E| = \frac{1}{2} \int_{-\infty}^{\infty}\int_{-\infty}^{\infty} (I\, \varepsilon^{jz\psi_{\varepsilon} jy\gamma} + I^{*}\, \varepsilon^{-jz\psi_{\varepsilon} - jy\gamma})\, dydz \tag{2-67}$$

The inverse of this amplitude pattern will yield the source distribution

$$i(y,z) = \frac{1}{2}\left[I(y,z) + I^{*}(-y,-z)\right] \tag{2-68}$$

We see again that use of the pattern magnitude only leads to an ambiguity in obstacle location. In this case the ambiguity is the reflection of the obstacle through the position of the dominant (antenna) element. As stated previously, a visual inspection can generally remove this ambiguity.

PREFACE TO CHAPTERS III AND IV

SYNTHESIS TECHNIQUES

As discussed in Chapter II, the whole theory of obstacle location depends on being able to uniquely determine the source currents producing a measured field pattern. Needless to say, this is not easily done because the mathematical relations involved in these general synthesis problems make most of them either impossible or unfeasible to solve. One-dimensional source problems, such as the linear array, are often exactly soluble. However, extensions to two- and three-dimensional sources are often plagued by field kernel functions which do not have the orthogonality properties over the visible range necessary for solution. This trouble occurs most frequently for arrays of discrete sources. Fortunately, the planar and circular source geometries pertinent to obstacle location on the Saturn can be systhesized subject to moderate restrictions or approximations.

To be covered in the next two chapters are the (1) linear, (2) circular, (3) planar, and (4) cylindrical source geometries. The linear and circular sources might be considered one-dimensional limiting forms of the cylinder. In the previous chapter the linear array and transform methods were treated in detail and, consequently, will only be briefly outlined in the next chapter for the sake of completeness.

CHAPTER III

ONE-DIMENSIONAL SOURCES

Linear Sources

The important results pertaining to a linear source geometry such as shown in Figure (3-1) will be briefly reviewed in this section.

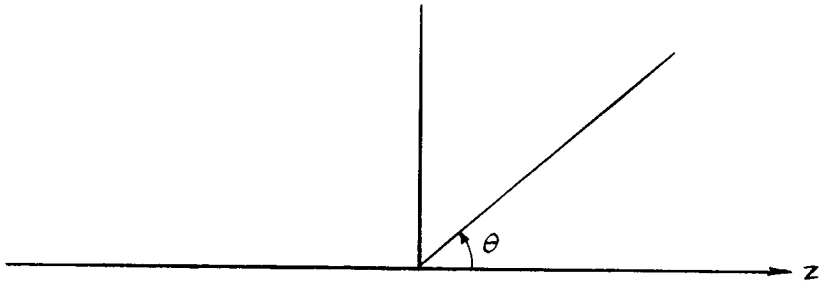

Figure 3-1 Linear Source Geometry

Fourier Transform for Linear Source

For a continuous line source coincident with the z-axis the isotropic far-field pattern simplifies to

$$E(\theta) = \int_{-\infty}^{\infty} I(z')e^{j\beta z' \cos\theta}\, dz' \qquad (3\text{-}1)$$

where $\beta = \frac{2\pi}{\lambda}$ = phase constant. As is shown in Chapter II, the current $I(z')$ is obtainable from

$$I(z') = \frac{1}{2\pi}\int_{-\infty}^{\infty} E(\theta)e^{-j\beta z' \cos\theta}\, d(\beta \cos\theta) \qquad (3\text{-}2)$$

where equations (3-1) and (3-2) are recognized as a Fourier transform pair. The band-limited problem due to truncation is also covered in Chapter II.

Fourier Series for a Line Array

The far-field pattern for an array of discrete sources is

$$E(\theta) = \sum_{-\infty}^{\infty} I_m e^{i\beta m d_z \cos\theta} \qquad (3\text{-}3)$$

By choosing $d_z = \frac{1}{2}\lambda$ equation (3-3) becomes

$$E(\theta) = \sum_{m=-\infty}^{\infty} I_m e^{im\pi \cos\theta} \tag{3-4}$$

The above is a complex Fourier series whose coefficients I_m are given by

$$I_m = \frac{1}{2\pi}\int_0^{\pi} E(\theta) e^{im\pi \cos\theta} \sin\theta \, d\theta \ . \tag{3-5}$$

Circular Ring Source

Consider the field due to similar sources (same directional characteristics) located on the circumference of the circle shown in Fig. 3-2.

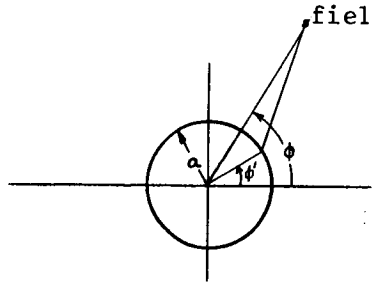

Fig. 3-2 Circular Source Geometry

The far-field radiation pattern is given for an array of discrete sources by

$$E(\phi) = G(\phi) \sum_{m=o}^{M} I_m e^{i\beta a \cos(\phi-\phi_m)} \tag{3-6}$$

or for a continuous distribution of current by

$$E(\phi) = G(\phi) \int_{-\pi}^{\pi} I(\phi') e^{i\beta a \cos(\phi-\phi')} \, d\phi' \ . \tag{3-7}$$

Mathematically the pseudo-isotropic function

$$f(\phi) = \frac{E(\phi)}{G(\phi)} \tag{3-8}$$

will be considered since the source or array factor $G(\phi)$ can be multiplied back once analysis is completed.

Unfortunately the sequence $\left\{e^{i\beta a \cos(\phi-\phi_m)}\right\}$ for the discrete source problem does not by itself nor with any known weighting function form an orthogonal system. As a consequence, Fourier series analysis which worked so nicely for linear arrays cannot be directly applied.

Nevertheless solutions do exist. The traditional approaches to the circular synthesis problem being (1) the Gram-Schmidt orthogonalization process, (2) a brute force matrix solution, and (3) a Bessel function approximation method. Also included in this report are some new — or possibly rediscovered — techniques, namely: (1) an integration, modified-matrix method, (2) an integration of a broadside pattern solution, and (3) a Fourier transform method.

Gram-Schmidt Orthogonalization Method

The Gram-Schmidt method is used to generate a sequence of orthonormal functions $\{O_n\}$ composed of a linear combination of the kernel functions $e^{i\beta \cos(\phi-\phi_m)}$.

Let this method be stated here in general terms for later reference in other synthesis problems. Given a sequence of functions (or vectors) $\{X_n\}=X_1,\ldots,X_n,\ldots$ for which the inner product denoted (X_n,X_m) has been defined [for a Fourier sine series the inner product denotes the integral operation $\int_{-\pi}^{\pi}\sin(mx)\sin(nx)\,dx = (X_m,X_n)$], the orthogonal set $\{U_n\}$ is produced by proper selection of the coefficients in the following equations:

$$
\begin{aligned}
U_1 &= X_1 \\
U_2 &= X_2 + a_{21}U_1 \\
U_3 &= X_3 + a_{31}U_1 + a_{32}U_2 \\
&\vdots \\
U_n &= X_n + \sum_{i=1}^{n-1} a_{ni}U_i \\
&\vdots
\end{aligned}
\qquad (3\text{-}9)
$$

To obtain the coeficients a_{ij} one successively applies the orthogonality condition

$$(U_m, U_n) = \begin{matrix} 0 & m \neq n \\ K \neq 0 & m = n \end{matrix} \qquad (3\text{-}10)$$

A concise statement of the Gram-Schmidt theory is given by the following two theorems:[4]

Theorem I. The functions (vectors) $x_1 \ldots x_n$ are linearly independent if and only if the Gramian

$$G_n = G(x_1, \ldots, x_n) = \begin{vmatrix} (x_1x_1) & (x_1x_2) & \cdots & (x_1x_n) \\ (x_2x_1) & & & \\ (x_3x_1) & & & \\ \vdots & & & \\ (x_nx_1) & & & (x_nx_n) \end{vmatrix} \neq 0 \qquad (3\text{-}11)$$

Theorem II. If $x_1, \ldots, x_n$ are linearly independent, then an orthogonal set $U_1, \ldots, U_n$ can be constructed by the determinants given in equations (3-12) below.

$$U_1 = x_1$$

$$U_2 = \begin{vmatrix} (x_1x_1) & x_1 \\ (x_2x_1) & x_2 \end{vmatrix}$$

$$U_3 = \begin{vmatrix} (x_1x_1) & (x_1x_2) & x_1 \\ (x_2x_1) & (x_2x_2) & x_2 \\ (x_3x_1) & (x_3x_2) & x_3 \end{vmatrix} \qquad (3\text{-}12)$$

$$\vdots$$

$$U_p = \begin{vmatrix} & & x_1 \\ & G_{p-1} & x_2 \\ & & \vdots \\ & & \vdots \\ (x_px_1) & \cdots & (x_px_{p-1}) \quad x_p \end{vmatrix}$$

The above orthogonal set can be normalized by letting

$$O_p = \frac{U_p}{\sqrt{G_p \, G_{p-1}}} \tag{3-13}$$

which makes

$$(O_m, O_n) = \delta_{mn} = \begin{cases} 1 & m=n \\ 0 & m \neq n \end{cases} \sim \text{Kronecker delta} \quad . \tag{3-14}$$

Once the orthonormal set $\{O_p\}$ has been constructed, a function f satisfying the Dirichlet conditions (see page 55) can be expanded as

$$f \sim \sum_{1}^{n} d_k O_k \tag{3-15}$$

in a truncated Fourier series where

$$d_k = (f, O_k) \quad . \tag{3-16}$$

The important quality of such an expansion is that both the truncated and infinite series are known to minimize the mean square error in describing f.

For the problem of the circular array it has been found convenient to define

$$\begin{aligned} x_0 &= e^{i\beta a \cos \phi} \\ x_1 &= e^{i\beta a \cos (\phi - \phi_1)} \\ &\vdots \\ x_n &= e^{i\beta a \cos (\phi - \phi_n)} \end{aligned} \qquad 0 = \phi_o < \phi_1 < \phi_2 < \ldots < \phi_n < 2\pi \tag{3-17}$$

and to choose for the inner product

$$(y_n, y_m) = \frac{1}{2\pi} \int_0^{\pi} y_n(\phi) y^*_m(\phi) \, d\phi \quad . \tag{3-18}$$

Occurring as terms in the determinants (3-12) will be

$$(x_n, x_m) = J_o\left[2\beta a \sin \frac{(\phi_n - \phi_m)}{2}\right]$$

$$(x_n, x_n) = 1.0 \quad .$$

Matrix Method

Another common method of solution is to solve via a digital computer the set of simultaneous equations formed by equating the actual field at discrete points to the assumed array. By picking M + 1 distinct values of $\tilde{\phi}$ the following M + 1 equations may be solved for that many unknowns I_m:

$$\begin{aligned} E(\tilde{\phi}_o) &= \sum_o^M I_m e^{i\beta a \cos(\tilde{\phi}_o - \phi_m)} \\ E(\tilde{\phi}_1) &= \sum_o^M I_m e^{i\beta a \cos(\tilde{\phi}_1 - \phi_m)} \\ &\vdots \\ E(\tilde{\phi}_M) &= \sum_o^M I_m e^{i\beta a \cos(\tilde{\phi}_M - \phi_m)} \end{aligned} \tag{3-19}$$

Equations (3-19) are expressible as the matrix

$$\begin{bmatrix} E(\tilde{\phi}_o) \\ \vdots \\ E(\tilde{\phi}_M) \end{bmatrix} = \begin{bmatrix} e^{i\beta a\cos\tilde{\phi}_o} & \cdots & e^{i\beta a\cos(\tilde{\phi}_o - \phi_M)} \\ e^{i\beta a\cos\tilde{\phi}_1} & & \vdots \\ \vdots & & \\ e^{i\beta a\cos\tilde{\phi}_m} & & e^{i\beta a\cos(\tilde{\phi}_M - \phi_M)} \end{bmatrix} \begin{bmatrix} I_o \\ I_1 \\ \vdots \\ I_M \end{bmatrix} . \tag{3-20}$$

The resultant currents I_m exactly reproduce the field at the chosen points $\tilde{\phi}_o, \ldots, \tilde{\phi}_M$. However, in the regions between the specified field points there is a sizable uncertainty unless a very large number of elements are used. But a computer solution of such a large order matrix, even using the advantageous Gauss' algorithm or Crout method for reduction of the matrix, presently is physically limited by the computer itself. The error accumulation and the switching times (affects total run time) of the best computers now available become intolerable for such large order systems. In a subsequent section the circular problem will be altered to give a coef-

ficient matrix which can be reduced to upper triangular form by hand and thereby greatly diminish the effects of the above faults.

Ksienski Approximate Method[5]

This is an integration method, and it depends on choosing the spacing between array elements so as to approximate the roots of the zero-order Bessel function $J_o(z)$. If $E(\phi)$ is expandable as

$$E(\phi) = \sum_{o}^{M} I_m e^{i\beta a \cos(\phi-\phi_m)} \quad , \tag{3-21}$$

then upon integration

$$F_p = \frac{1}{2\pi} \int_{o}^{2\pi} E(\phi) e^{-i\beta a \cos(\phi-\phi_p)} d\phi = \sum_{o}^{M} I_m J_o\left[2\beta a \sin \frac{(\phi_m - \phi_p)}{2} \right] \tag{3-22}$$

By selecting array points to linearize

$$\sin\left[\frac{\phi_p - \phi_m}{2}\right] = j/J$$

the choice

$$a = \text{array radius} = \frac{2.9\,J}{4\pi}\,\lambda$$

corresponding to $2\beta a/J = 2.9$ is seen to make $J_o\left[2\beta a \sin\left(\frac{\phi_p - \phi_m}{2}\right)\right]$ nearly vanish except for p = m. Multiples of 2.9 give

x =	0.0	2.9	5.8	8.7	11.6
$J_0(x)$	1.000	-.224	+.092	-.012	-.045

. (3-23)

Ksienski stretched his imagination to infer that

$$J_o\left[2\beta a \sin \frac{\phi_p - \phi_m}{2}\right] \quad \begin{matrix} \approx 0 & p \neq m \\ = 1 & p = m \end{matrix} \tag{3-24}$$

and hence

$$I_m \approx F_m = \frac{1}{2\pi} \int_0^{2\pi} E(\phi)\, e^{-i\beta a \cos(\phi-\phi_m)}\, d\phi \ . \qquad (3\text{-}25)$$

As is evident from the values in (3-23), false source elements would be detected in the neighborhood of an actual source and these could have magnitudes up to 22% of the true element. Note that the choice of 2.9 is a minimum optimum value that was picked by scanning a table of zero-order Bessel functions. A slightly better maximum error figure of 18% is obtainable by using 2.8, but this value has a disadvantage that 2.9 does not have in that it gives relatively large errors for elements far distant from the true source. In other words, the 2.9 figure concentrates its error in the elements adjacent to the real one and thus the general vicinity of an actual source is strongly indicated by this approximation. This is not the case for some of the other choices. Obviously the presence of such large order error means that this method is of little worth for critical synthesis work where a particular pattern has to be reproduced by the generated array. However, the 2.9 approximation in (3-34) improves for larger multiples implying that this method could be effectively used to show the general proximity of a significant disturbance in obstacle location. Again 2.9 determines a minimum radius. If larger radii are permitted, an improved error may be obtained by using a multiple of 2.9 as the basic factor (10% maximum error for instance with 5.8).

Simplified Matrix Solution for Circular Array Problem

Both the Gram-Schmidt and matrix methods already mentioned are extremely lengthy and error prone for very large order systems. As a result of this research, an alternate digital computer method has been developed which is quick and highly accurate compared to the above named techniques.

Recall for the circular array of isotropic point sources, the far-field pattern is

$$E(\phi) = \sum_{m=0}^{M} I_m e^{i\beta a \cos(\phi-\phi_m)} \tag{3-26}$$

Next, consider the Fourier series expansion of a given radiation pattern

$$E(\phi) = \sum_{-\infty}^{\infty} B_n \varepsilon^{in\phi} \tag{3-27}$$

where

$$B_n = \frac{1}{2\pi} \int_0^{2\pi} E(\phi) e^{-in\phi} d\phi \ . \tag{3-28}$$

Let it be assumed that enough array points $\phi' = \phi_m = m\frac{2\pi}{M+1}$ uniformly distributed on the ring are chosen so that the series in Equation (3-26) can be used to represent the field in (3-27). Then

$$B_n = \frac{1}{2\pi} \int_0^{2\pi} \sum_{m=0}^{M} I_m \varepsilon^{i\beta a \cos(\phi-\phi_m)-in(\phi)} d\phi$$

$$= i^n J_n(\beta a) \sum_{m=0}^{M} I_m \varepsilon^{-inm\Delta\phi} \tag{3-29}$$

Clearly, for an arbitrary $E(\phi)$ an acceptable value of M would be determined by the integer N which would keep the truncated version of (3-27)

$$E_t(\phi) = \sum_{-N}^{N} B_n \varepsilon^{in\phi} \tag{3-30}$$

within a specified error bound. All physically occurring patterns are continuous and hence are known to coverage uniformly. Since uniform convergence of a Fourier series implies rapid convergence and no Gibb's phenomenon, truncation is easily justified. Thus the logical choice is M = 2N. Now

if the quantity C_n is defined

$$C_n \triangleq \frac{B_n}{i^n J_n(\beta a)} = \frac{\int_0^{2\pi} E(\phi) e^{-in\phi}\, d\phi}{2\pi\, i^n\, J_n(\beta a)} \tag{3-31}$$

and provided, of course, $J_n(\beta a) \neq 0$, the correspondence

$$C_n = \sum_{m=o}^{M} I_m \varepsilon^{-imn\,\Delta\phi} \quad , \; n = 0, \pm 1, \pm 2, \ldots, \pm N, \tag{3-32}$$

is obtained. It is this system of equation (3-32) which offers an attractive solution to the problem.

To solve, the equations (3-32) are first put in matrix form $[C] = [M]\,[I]$:

$$\begin{bmatrix} C_{-N} \\ \vdots \\ C_{-1} \\ C_o \\ C_1 \\ \vdots \\ C_N \end{bmatrix} = \begin{bmatrix} 1 & e^{iN\Delta} & \cdots & e^{iMN\Delta} \\ \vdots & & & \\ 1 & e^{i\Delta} & e^{2i\Delta} \cdots & e^{iM\Delta} \\ 1 & 1 & 1 \cdots & 1 \\ 1 & e^{-i\Delta} & \cdots & \\ \vdots & & & \\ 1 & & & e^{-iMN\Delta} \end{bmatrix} \begin{bmatrix} I_o \\ I_1 \\ \vdots \\ \\ \\ \\ I_M \end{bmatrix} \tag{3-33}$$

If the matrix $[M]$ is non-singular ($\det|M| \neq 0$), the required solution could be given by $[I] = [M]^{-1}\,[C]$ where $[M]^{-1}$ denotes the inverse of the matrix $[M]$. However, for a digital computer solution there exists a much more efficient means of solution, namely, Gauss' algorithm.

The basis of the Gauss method is a reduction of the coefficient matrix $[M]$ to upper triangular form $[M']$ (all zeros below the main diagonal) by performing elementary row manipulations. From the theory of matrices[6], it is known that the solutions of the original matrix equation

$$[C] = [M][I]$$

will be equivalent to the upper triangular system

$$[C'] = [M'][I]$$

provided the column $[C]$ undergoes the same row operations that were exercised in reducing $[M]$ to $[M']$.

The advantages claimed for this particular matrix method result from the fact that the matrix $[M]$ in equation (3-33) is so well behaved that the authors have been able to reduce it to the desired upper triangular form by hand. Let the types of operations used in the aforementioned algorithm be illustrated by repeating the first few steps used on $[M]$. Starting with

$$[M] = \begin{bmatrix} 1 & e^{iN\Delta} & e^{i2N\Delta} & e^{i3N\Delta} & \cdots & e^{iMN\Delta} \\ 1 & e^{i(N-1)\Delta} & e^{i2(N-1)\Delta} & e^{i3(N-1)\Delta} & \cdots & \\ 1 & e^{i(N-2)\Delta} & e^{i2(N-2)\Delta} & e^{i3(N-2)\Delta} & & \\ \vdots & & & & & \\ 1 & e^{i\Delta} & e^{i2\Delta} & e^{i3\Delta} & \cdots & e^{iM\Delta} \\ 1 & 1 & 1 & 1 & \cdots & 1 \\ 1 & e^{-i\Delta} & e^{-i2\Delta} & e^{-i3\Delta} & & \\ \vdots & & & & & \\ 1 & e^{-iN\Delta} & \cdots & & & e^{-iMN\Delta} \end{bmatrix} \qquad (3\text{-}34)$$

The first row is subtracted from all subsequent rows, and from the second row down the elements in the second column are normalized by dividing their rows by the appropriate factors.

$$\begin{bmatrix} 1 & e^{iN\Delta} & e^{i2N\Delta} & e^{i3N\Delta} & \cdots \\ 0 & 1 & e^{i(N-1/2)\Delta}\,\frac{\sin\Delta}{\sin(\Delta/2)} & e^{i2(N-1/2)\Delta}\,\frac{\sin(3\Delta/2)}{\sin(\Delta/2)} & \cdots \\ 0 & 1 & e^{i(N-3/2)\Delta}\,\frac{\sin\Delta}{\sin(\Delta/2)} & \cdots & \\ 0 & 1 & \cdots & & \\ 0 & 1 & & & \\ \vdots & \vdots & & & \\ 0 & 1 & & & \end{bmatrix} \tag{3-35}$$

Next the second row is subtracted from succeeding rows and the new elements in the third column are normalized by proper row division.

$$\begin{bmatrix} 1 & e^{iN\Delta} & e^{i2N\Delta} & e^{i3N\Delta} & \cdots \\ 0 & 1 & e^{i(N-1/2)\Delta}\,\frac{\sin\Delta}{\sin(\Delta/2)} & e^{i2(N-1/2)\Delta}\,\frac{\sin(3/2)\Delta}{\sin(\Delta/2)} & \cdots \\ 0 & 0 & 1 & e^{i(N-1)\Delta}\,\frac{\sin(3\Delta/2)}{\sin(\Delta/2)} & \\ 0 & 0 & 1 & & \\ \vdots & \vdots & \vdots & & \\ 0 & 0 & 1 & & \end{bmatrix} \tag{3-36}$$

The above process is repeated until the matrix is in upper triangular form M' :

$$[M'] = \begin{bmatrix} 1 & e^{iN\Delta} & e^{i2N\Delta} & e^{i3N\Delta} & e^{i4N\Delta} & \cdots \\ 0 & 1 & & & & \\ 0 & 0 & 1 & & & \\ 0 & 0 & 0 & 1 & & \\ 0 & 0 & 0 & 0 & 1 & \\ \vdots & & & & & \\ 0 & 0 & 0 & 0 & 0 \;\cdots & 1 \end{bmatrix} = (m'_{ij}) \tag{3-37}$$

where $m'_{jj} = 1.00$

$$m'_{j,\,j+k} = e^{ik\left(\frac{M+1-j}{2}\right)\Delta}\,\frac{\sin\left(j+k-1\right)\frac{\Delta}{2}\,\sin\left(j+k-2\right)\frac{\Delta}{2}\cdots\,\sin\left(\frac{k+1}{2}\Delta\right)}{\sin\frac{\Delta}{2}\,\sin\Delta\,\sin\frac{3}{2}\Delta\,\cdots\,\sin\frac{j-1}{2}\Delta} \quad (k > 0)$$

By inspection M' is non-singular, and hence the solution exists. The justification for the Gauss reduction is made readily obvious by the simple addition and subtraction steps that are all that are required to determine the solutions to the new matrix equation

$$\begin{bmatrix} C'_{-N} \\ \cdot \\ \cdot \\ \cdot \\ C'_{-1} \\ C'_{0} \\ C'_{1} \\ \cdot \\ \cdot \\ C'_{N} \end{bmatrix} = \begin{bmatrix} 1 & e^{iN\Delta} & e^{i2N\Delta} & \cdots & e^{iMN\Delta} \\ 0 & 1 & & & \\ 0 & 0 & 1 & & \\ \vdots & & & & \\ & & & 0\ 1 & m'_{M-1,M} \\ 0 & 0 & 0 \cdots\cdots 0 & & 1 \end{bmatrix} \begin{bmatrix} I_0 \\ I_1 \\ \\ \\ \\ \\ I_{M-1} \\ I_M \end{bmatrix} \qquad (3\text{-}38)$$

As applied to (3-38), the last row gives

$$I_M = C'_{M/2} = C'_N \quad .$$

Now I_M is known and may be used in the next to last row to find

$$I_{M-1} = C'_{N-1} - m'_{M-1,M}\, I_M$$

The procedure is similarly continued, each time moving up a row until all the unknowns I_m have been ascertained. No large order determinants need ever be evaluated.

Now let us consider the merits of the above solution of the altered matrix problem $[C] = [M][I]$. By being able to reduce $[M]$ to $[M']$ in advance, there is no time wasted and no error built up in performance of a computer reduction. The magnitude of the problem is shown by considering the reduction of an NxN matrix. For such a matrix, on the order of $(N-1)^2 + (N-2)^2 + \ldots + 2^2 + 1^2 = \frac{N(N-1)\,(2N-1)}{6}$ steps are required in the reduction. The cubic dependence on N for large N emphasizes the great time savings afforded by being able to program $[M']$ directly. As for the error accumulation, this is a consequence of having rows with newly introduced error operate on other rows. For small order matrices this is not serious, but for a matrix of

rank say 1000 considerable error is compounded by the time the error in the first row is transmitted to all the rest, then the possibly increased error in the second row is transferred to succeeding rows, and so on until finally the thousandth row is reached — it could theoretically be as bad as 2^{999} x error of a particular element in computer storage. To be sure, knowing (M') in advance puts the error figure right back where it should be, limited only by the computer element capacity.

Broadside Pattern Integration for Circular Array

An exact integration method is applicable to a circular ring array if the data points are measured or specified in a plane perpendicular to the plane of the ring.

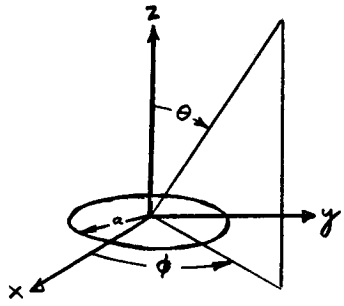

Fig. 3-3 Circular Array, Broadside Pattern

In other words a broadside pattern $E(\theta,\phi=0)$ can be produced by a circle of discrete sources. Referring to the geometry and orientation in Fig. 3-3, the isotropic far-field is

$$E(\theta,\phi) = \sum_{o}^{M} I_m e^{ika\cos(\phi-\phi_m)\sin\theta} \qquad (3\text{-}39)$$

Inspection of equation (3-39) shows that choosing $\phi=0$ gives

$$E(\theta,0) = \sum_{o}^{M} I_m e^{ika\sin\theta\cos\phi_m} \qquad (3\text{-}40)$$

Now considering

$$F_q = \int_{-\pi/2}^{\pi/2} E(\theta,0)\, e^{ika\, \sin\theta\, \cos\phi_q}\, \cos\theta\, d\theta \qquad (3\text{-}41)$$

gives

$$F_q = 2\sum_{o}^{M} I_m \frac{\sin\{ka(\cos\phi_m - \cos\phi_q)\}}{ka(\cos\phi_m - \cos\phi_q)} \quad . \qquad (3\text{-}42)$$

In light of the $\frac{\sin\{ka(\cos\phi_m - \cos\phi_q)\}}{ka(\cos\phi_m - \cos\phi_q)}$ terms in (3-42) we see that they may be made zero except for m=q by wise choice of array points ϕ_m and array radius. By selecting ϕ_m such that

$$\cos\phi_m = \frac{M-m}{M} \quad (m = 0, 1, \ldots, 2M)$$

and the making

$a = \frac{M}{2}$ wavelengths (or integer multiples thereof) we get

$$\frac{\sin\{ka\,(\cos\phi_m - \cos\phi_p)\}}{ka(\cos\phi_m - \cos\phi_p)} = \frac{\sin\{(p-m)\pi\}}{(p-m)\pi} = \begin{matrix} 0 & p\neq m \\ 1 & p=m \end{matrix} \quad .$$

Since all the terms in the summation (3-42) now vanish except the qth,

$$I_m = \frac{F_m}{2} \quad . \qquad (3\text{-}43)$$

Band-limited Transform for Circular Synthesis

Of academic appeal is a transform solution to the circular problem which was noticed by the authors. In integral form

$$E(\phi) = \int_{-\pi}^{\pi} I(\phi')e^{i\beta a\, \sin(\phi-\phi')}\, d\phi' \qquad (3\text{-}44)$$

Note that there is no real change in the problem by using the $\sin(\phi-\phi')$ term in place of $\cos(\phi-\phi')$ because it is just a matter of measuring ϕ' from

the -y-axis or letting $\phi'_{new} = \phi'_{old} - \pi/2$. As will be seen below, this is done to help simplify the transform of the kernel function.

The transforms to be used are a band-limited Fourier transform pair

$$\tilde{F}(\omega) = \mathcal{F}\left[f(t)\right] = \frac{1}{2\pi} \int_{-\pi}^{\pi} f(t)e^{-j\omega t}dt \tag{3-45}$$

$$f(t) = \mathcal{F}^{-1}\left(\tilde{F}(\omega)\right) = \int_{-\infty}^{\infty} \tilde{F}(\omega)e^{+j\omega t}d\omega. \tag{3-46}$$

Those familar with Fourier transform theory will recognize the assumption that is implied by equation (3-45), which is that f(t) be zero outside of the band $(-\pi,\pi)$. Consideration of (3-44) shows that this band limitation is not overly restrictive since it simply means that only one periodic interval will be utilized to describe the periodic source, kernel, or field functions. Actually inclusion of more than one periodic cycle would not yield any new information and would in most cases cause bad convergence and interpretation problems if used in the infinite version of (3-45). In order to avoid the uniqueness and existence dilemmas created by band-limiting in both domains (see Chapter II), it will also be assumed that $\tilde{F}(\omega)$ is not band-limited. Then it follows that the preceding transform pair is unique.

Returning to the problem, let us take the finite transform of $E(\phi)$ as expressed in (3-44)

$$\tilde{E}(\omega) = \frac{1}{2\pi} \int_{-\pi}^{\pi} E(\phi)e^{-j\omega\phi}d\phi =$$

$$\frac{1}{2\pi} \int_{-\pi}^{\pi} e^{-j\omega\phi}d\phi \int_{-\pi}^{\pi} I(\phi')e^{i\beta a \sin(\phi-\phi')}\, d\phi' \tag{3-47}$$

Both integrals are obviously uniformly convergent so order of integration may be changed giving

$$\tilde{E}(\omega) = \frac{1}{2\pi} \int_{-\pi}^{\pi} I(\phi') e^{-i\phi'\omega} d\phi' \int_{-\pi}^{\pi} e^{i\beta a \sin(\phi-\phi') - i\omega(\phi-\phi')} d(\phi-\phi')$$

which expresses

$$\tilde{E}(\omega) = 2\pi \tilde{I}(\omega) \tilde{K}(\omega) \quad . \tag{3-48}$$

In the above $\tilde{K}(\omega)$ is by definition the transform of the kernel function:

$$\tilde{K}(\omega) \triangleq \mathcal{F}\left[e^{i\beta a \sin\alpha}\right] = \frac{1}{2\pi} \int_{-\pi}^{\pi} e^{i\beta a \sin\alpha - i\omega\alpha} d\alpha .$$

From (3-48) it is seen that

$$\tilde{I}(\omega) = \frac{\tilde{E}(\omega)}{2\pi \tilde{K}(\omega)} \quad , \tag{3-49}$$

and hence

$$I(\phi') = \text{Inverse}\left[\tilde{I}(\omega)\right] = \int_{-\infty}^{\infty} \frac{\tilde{E}(\omega)}{2\pi \tilde{K}(\omega)} e^{+j\phi'\omega} d\omega \quad . \tag{3-50}$$

As the kernal function is known, its transform will be evaluated and directly inserted in the above. There are basically two analytic forms in which $\tilde{K}(\omega)$ can be expressed:

$$\text{(A)} \qquad \tilde{K}(\omega) = \frac{1}{2\pi} \int_{-\pi}^{\pi} e^{i\beta a \sin\alpha - i\omega\alpha} d\alpha \triangleq A_{\omega}(\beta a) \tag{3-51}$$

$$\text{where } A_{\alpha}(\beta a) \triangleq \text{Anger function} \triangleq \frac{1}{\pi} \int_{0}^{\pi} \cos(\alpha\theta - \beta a \sin\theta)\, d\theta \tag{3-52}$$

Observe that for α = integer the integral (3-52) is Bessel's integral and $A_{\alpha}(f)$ reverts to a Bessel function $J_n(f)$.

$$\text{(B)} \qquad \tilde{K}(\omega) = \sum_{-\infty}^{\infty} J_n(\beta a) \frac{\sin\{(n-\omega)\pi\}}{(n-\omega)\pi} \tag{3-53}$$

where $J_n(\beta a)$ denotes the nth-order Bessel function. The expression (3-53) follows from using the expansion

$$e^{iz\sin\phi} = \sum_{-\infty}^{\infty} J_n(z)\, e^{in\phi} \tag{3-54}$$

in the definition of $\tilde{K}(\omega)$

$$\tilde{K}(\omega) = \frac{1}{2\pi}\int_{-\pi}^{\pi}\sum_{-\infty}^{\infty} J_n(\beta a)e^{in\alpha - i\omega\alpha}\, d\alpha =$$

$$\sum_{-\infty}^{\infty} J_n(\beta a)\,\frac{\sin((n-\omega)\pi)}{(n-\omega)\pi} \quad .$$

Using the notationally simpler form of $\tilde{K}(\omega)$, equation (3-50) may then be written

$$I(\phi') = \int_{-\infty}^{\infty}\frac{\tilde{E}(\omega)e^{i\omega\phi'}}{2\pi\, A_\omega(\beta a)}\, d\omega \quad . \tag{3-55}$$

The real test of this method is in its application to practical problems as will be illustrated by the two examples to follow:

Example 1- Consider the far-field produced by isotropic point sources

$$E(\phi) = \sum_{0}^{M} B_m e^{i\beta a\sin(\phi-\phi_m)}$$

Its transform is

$$\tilde{E}(\omega) = \frac{1}{2\pi}\int_{-\pi}^{\pi}\sum_{0}^{M} B_m e^{i\beta a\sin(\phi-\phi_m) - i\omega\phi}\, d\phi$$

$$= \sum_{0}^{M} B_m\, A_\omega(\beta a)e^{-i\omega\phi_m}$$

Then

$$I(\phi') = \frac{1}{2\pi} \int_{-\infty}^{\infty} \frac{B_m \cancel{A_\omega(\beta a)} \varepsilon^{-i\omega\phi_m + i\omega\phi'}}{\cancel{A_\omega(\beta a)}} d\omega$$

$$= \sum_{o}^{M} B_m \delta(\phi' - \phi_m)$$

which is just as expected.

Example 2 A more difficult example that was solved was for the pattern

$$E(\phi) = \sin\phi$$

Transformed

$$\tilde{E}(\omega) = \frac{1}{2\pi} \int_{-\pi}^{\pi} \frac{e^{i\phi} - e^{-i\phi}}{2i} e^{-i\omega\phi} d\phi = \frac{1}{4\pi i} \left\{ \frac{e^{i\phi(1-\omega)}}{i(1-\omega)} \Big/_{-\pi}^{\pi} - \frac{e^{-i\phi(1+\omega)}}{-i(1+\omega)} \Big/_{-\pi}^{\pi} \right\}$$

$$= \frac{1}{2\pi i} \left[\frac{\sin \pi(1-\omega)}{(1-\omega)} + \frac{\sin \pi(1+\omega)}{-(1+\omega)} \right]$$

Solving gives

$$I(\phi') = \frac{1}{2\pi} \int_{-\infty}^{\infty} \frac{E(\omega)}{A_\omega(\beta a)} e^{i\omega\phi'} d\omega = \frac{1}{2\pi} \frac{1}{2i} \int_{-\infty}^{\infty} \left[\frac{\sin \pi(1-\omega)}{\pi(1-\omega)} - \frac{\sin \pi(1+\omega)}{\pi(1+\omega)} \right] \frac{e^{i\omega\phi'}}{A_\omega(\beta a)} d\omega$$

$$= \frac{1}{4\pi i} \left[\frac{e^{i\phi'}}{A_1(\beta a)} + \frac{-e^{-i\phi'}}{A_{-1}(\beta a)} \right] = \frac{1}{2\pi i J_1(\beta a)} \cos\phi'$$

It should be clear by now that this method is a useful theoretical technique, however, for obstacle location it has its drawbacks. First the integral (3-55) is an infinite one not always suitable for computerization or analytic solution. Also to evaluate that integral, $\tilde{E}(\omega)$ must be known for an infinite range of the variable ω. This knowledge, as experience shows, is not easily obtainable unless $E(\phi)$ is given as an exact mathematical expression which can be used in (3-47). As with several other synthesis techniques which require explicit mathematical formulations, this process

finds little use for data dependent obstacle location.

CHAPTER IV

TWO-DIMENSIONAL SOURCES

The tools of mathematical analysis have lent themselves nicely to the analysis of synthesis problems involving one-dimensional sources, unfortunately such is not always the case for two-dimensional sources — at least not for the obstacle problem where the field is described only by data points taken over the visible region. As will be seen, exact methods of synthesis do exist, however they are generally incalculably large for obstacle location. It is common to find, even with the aid of a large high-speed digital computer, that the two-dimensional synthesis problem is of such functional complexity and dimensional magnitude that exact solutions must be abandoned in favor of approximations. One such approximate method for the cylindrical array is highly advantageous and is accordingly recommended.

Although theoretically possible, neither the Gram-Schmidt nor the brute force matrix methods will be used in this chapter since both are unmanageably large order systems. For instance, the orthogonalization process has to evaluate determinants up to and including rank $(2N+1)^2$ as compared to a maximum rank of (2N+1) for the one-dimensional case. Similarly a matrix of order (2N+1) (2M+1) is now involved, whereas for the one-dimensional source it was of rank (2N+1). Finally in addition to the time required and the error compounded in a computer solution, many present computers lack sufficient variable locations to even store the matrix needed to solve the two-dimensional problem.

Examined in this chapter are the planar and cylindrical sources. The planar source is included because in locating obstacles on a vehicle it is suspected that much of the reradiation could be confined to an arc

with protruding objects (fins, etc.) which for many purposes might be approximated by a plane. Naturally the cylindrical source needs little justification for its inclusion since it best resembles the actual structure of contemporary launch vehicles. Consequently, much of this work was concentrated on the cylindrical configuration, and it happily led to some rather useful results.

In conjunction with the subsequent methods for discrete cylindrical arrays, several of them will have solutions which depend on a restricted choice of array radius. Actually this is not a serious limitation because, if the solution radius does not coincide with the true one, it is always possible to approximate the important regions of the true source by inscribing it inside a larger radius cylinder. The larger cylinder must satisfy the radius condition for array solvability and be tangent to the existent array on the line containing the dominant central antenna point.

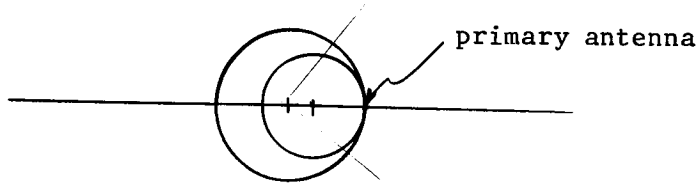

Fig. 4-1

As suggested by Fig. 4-1, this simulation should prove especially valuable for original arrays of large wavelength radii where the true and approximate can be made nearly alike over the important 90° section containing the primary antenna.

Rectangular Source Geometry

Dual Fourier Series

For a rectangular array in the xz-plane the isotropic far-field pat-

tern is

$$E(\theta,\phi) = \sum_{-\infty}^{\infty}\sum_{-\infty}^{\infty} I_{mn} e^{i\beta n d_z \cos\theta + i\beta m d_x \sin\theta \cos\phi} \qquad (4\text{-}1)$$

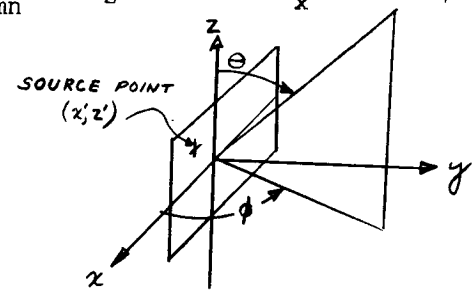

Fig. 4-2 Rectangular Source

The coefficients in the above series may be found if the precise mathematical formulation for $E(\theta,\phi)$ is known and it satisfies the Dirichlet conditions (see page). Under these circumstances the substitutions $u=\cos\theta$ and $v=\sin\theta\cos\phi$ (or what is equivalent, the projection of the pattern $E(\theta,\phi)$ $(y>0)$ first onto a unit hemisphere and then onto a unit circle in the xz-plane) puts equation (4-1) in a form more suitable for solution. By choosing the elemental array spacings $d_x = 1/2\ \lambda$ and $d_z = 1/2\ \lambda$, equation (4-1) becomes

$$E(u,v) = \sum_{-\infty}^{\infty}\sum_{-\infty}^{\infty} I_{mn} e^{in\pi u + in\pi v} . \qquad (4\text{-}2)$$

Then the coefficients are given by

$$I_{mn} = \left(\frac{1}{2\pi}\right)^2 \int_{-1}^{1}\int_{-1}^{1} E(u,v)\, e^{-in\pi u - im\pi v}\, du\,dv \qquad (4\text{-}3)$$

The above is almost trivial, but in obstacle location no such explicit field expression is available, and hence the method cannot be applied.

Dual Fourier Transform Method

As shown in Chapter II the far-field pattern and source function

$I(x',z')$ may also be represented as a Fourier transform pair

$$E(\theta,\phi) = \int_{-\infty}^{\infty}\int_{-\infty}^{\infty} I(x',z')e^{i\beta z' \cos\theta + i\beta x' \sin\theta \cos\phi} \, dx' \, dz' \tag{4-4}$$

$$I(x',z') = \left(\frac{1}{2\pi}\right)^2 \int_{-\infty}^{\infty}\int_{-\infty}^{\infty} E(\theta,\phi)e^{-\beta z' \cos\theta - i\beta x' \sin\theta \cos\phi} \, d(\beta\cos\theta) \, d(\beta \sin\theta \cos\phi) \tag{4-5}$$

Defining

$$u = \beta \cos\theta$$
$$v = \beta \sin\theta \cos\phi \tag{4-6}$$

gives

$$E(u,v) = \int_{-\infty}^{\infty}\int_{-\infty}^{\infty} I(x',z')e^{iz'u + ix'v} \, dx'dz' \tag{4-7}$$

$$I(x',z') = \left(\frac{1}{2\pi}\right)^2 \int_{-\infty}^{\infty}\int_{-\infty}^{\infty} E(u,v)e^{-iz'u - ix'v} \, dudv \tag{4-8}$$

This method also gives an exact solution, but it requires knowledge of the invisible region ($|\cos\theta| > 1$) in order to solve for $I(x',z')$. For finite sources, as are always found in practice, the same band-limiting problem arises for two-dimensional sources as did in the line source problem discussed earlier. Note that this method would work if $E(\theta,\phi)$ were mathematically specified and the integral (4-8) properly existed. Of course, an analytic expression for $E(\theta,\phi)$ is not available in data oriented obstacle location, nor can data be taken for the invisible region.

There is, however, a clever way to use the band-limited property of $I(x',z')$, namely, Woodward's method to be treated next.

Woodward's Method[7]

Assume

(A) the rectangular source region is finite of width W and length L.

(B) the source function satisfies the Dirichlet conditions: it is sectionally continuous with at worst a finite number of finite discontinuities, is bounded, is periodic, and has a finite number of maxima and minima.

The source to be used in this section is shown in Fig. 4-3.

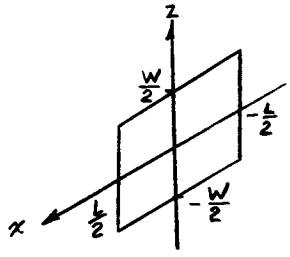

Fig. 4-3 Finite Rectangular Source Distribution

By virtue of condition (B), $I(x',z')$ may be expanded in a dual Fourier series with periods W and L

$$I(x',z') = \sum_{-\infty}^{\infty} \sum_{-\infty}^{\infty} a_{mn} \varepsilon^{-jx'n\Delta x - jz'm\Delta z} \tag{4-9}$$

where

$$\Delta x = \frac{2\pi}{L} \text{ and } \Delta z = \frac{2\pi}{W} .$$

Integrating $I(x',z')$ yields the far-field pattern

$$E(\theta,\phi) = \int_{-L/2}^{L/2} \int_{-W/2}^{W/2} I(x',z') e^{ikx' \sin\theta \cos\phi + ikz' \cos\theta} dz'dx' \tag{4-10}$$

Substituting the expansion (4-9) into (4-10) and evaluating the integral gives

$$E(\theta,\phi) = \sum_{-\infty}^{\infty}\sum_{-\infty}^{\infty} WL\, a_{mn} \frac{\sin\left[(k\sin\theta\cos\phi - n\Delta x)\frac{L}{2}\right]}{\frac{L}{2}(k\sin\theta\cos\phi - n\Delta x)} \frac{\sin\left[\frac{W(k\cos\theta - m\Delta z}{2}\right]}{\frac{W}{2}(k\cos\theta - m\Delta z)} \quad (4\text{-}11)$$

By letting $\begin{cases} v = k\sin\theta\cos\phi \\ u = k\cos\theta \end{cases}$ it is seen that $E(\theta,\phi) \longrightarrow E(u,v)$

and $$a_{mn} = E\left(u = \frac{2\pi m}{W},\ v = \frac{2\pi n}{L}\right)/WL \quad (4\text{-}12)$$

Of all the synthesis methods for rectangular sources Woodward's method is probably the simplest and most productive. In the physical world conditions (A) and (B) are always satisfied, and it is therefore logical to apply this method. There are, however, certain pitfalls which must be carefully examined and avoided.

For one, consider the far-field expression

$$E(\theta,\phi) = \sum\sum I_{mn}\varepsilon^{in\pi\cos\theta + im\pi\sin\theta\cos\phi}$$

which corresponds to discrete point sources at $x' = \frac{m}{2}\lambda$ and $z' = \frac{n}{2}\lambda$. The current distribution $I(x',z')$ necessary for equation (4-10) to give the above pattern would be $I(x',z') = \sum\sum I_{mn}\,\delta(x' - \frac{m}{2})\,\delta(z' - \frac{n}{2})$. Noting the presence of the Dirac-delta functions it is seen that condition (B) rules out the existence of the required Fourier series.

One then says if point sources are ruled out let them be replaced by pulses of finite width. At first this requirement may also seem too severe since physically the source must be continuous. However, in obstacle location it is common to deal with a relatively large magnitude source concentrated in an extremely small area. This means the slope of the sides of the continuous function for all practical purposes is great enough to approximate a discontinuity, especially when viewed relative

to the total source region W by L. As a consequence, the pulses will be treated as a worst case to often be approached in reality.

Inherent in the Fourier series representation of discontinuous functions such as pulses is the Gibb's phenomenon. Recall for the one-dimensional case the truncated series for f(x) is given by

$$S_N(x) = \frac{A_o}{2} + \sum_{n=1}^{N} A_n \cos(nx) + B_n \sin(nx) \tag{4-14}$$

which by a trigonometric identity is equivalent to

$$S_N(x) = \int_0^{2\pi} f(x-t) \frac{\sin(N + \frac{1}{2})t}{2\pi \sin \frac{t}{2}} dt \tag{4-15}$$

If f(x) satisfies the Dirichlet conditions, then $\lim_{N \longrightarrow \infty} S_N(x) = \frac{1}{2}\left[f(x^+) + f(x^-)\right]$.

Gibb's phenomenon states that near discontinuities in f, the truncated series even for large N does not necessarily converge to f(x). Davis concludes that for sufficiently large N the truncation error is less than 9% of the discontinuity.[8] Optimum selection of N for truncation of the series for a pulse of width Δ is dictated by the bandwidth of the Dirichlet kernel

$$D_N(t) = \frac{\sin (N + \frac{1}{2})t}{2\pi \sin \frac{t}{2}} . \tag{4-16}$$

If Δ is the desired source resolution for the finite series, than a suitable choice for the integer N is determined by

$$\frac{2\pi}{N} < \Delta \tag{4-17}$$

Visually this is apparent for the one-dimensional series by observing the convolution form exhibited in equation (4-15).

Figure 4-4 Dirichlet Kernels

As graphically shown in Figure 4-4 it is obvious that the wider bandwidth kernel gives a significant value to the convolution in (4-15) for x far exterior to the actual pulse. The inequality (4-17) makes detection ambiguous only for a range of about $\Delta/2$.

Rectangular Array by Numerical Integration

Contained in this section is a solution for a two-dimensional rectangular array of point sources employing numerical integration and relying on a proper choice of element spacing. For an xz-planar array with $d_z = \frac{1}{2}\lambda$ and d_x to be determined, the isotropic far-field pattern is given by

$$E(\vartheta,\phi) = \sum_{-M}^{N}\sum_{-N}^{N} I_{mn}\varepsilon^{in\pi\cos(\vartheta) + im\beta\, d_x \cos\phi\, \sin\vartheta} \qquad (4\text{-}18)$$

Defining

$$F_p(\vartheta) = \int_0^{\pi} E(\vartheta,\phi)\, \varepsilon^{-ip\beta d_x \sin\vartheta \cos\phi} \sin\phi\, d\phi \qquad (4\text{-}19)$$

it is seen by substituting equation (4-18) into (4-19) that

$$F_p(\vartheta) = 2\sum_{-M}^{M}\sum_{-N}^{N} I_{mn}\varepsilon^{in\pi\cos\vartheta}\, \frac{\sin\{\beta d_x(m-p)\sin\vartheta\}}{\beta d_x(m-p)\sin\vartheta} \; . \qquad (4\text{-}20)$$

The points θ_j to be used in the subsequent numerical integration are then chosen to linearize

$$\sin\theta_j = \frac{j}{J} \quad (0,\pi/2)$$

Now by making $d_x = \frac{1}{2}J$ the sin(x)/(x) terms in equation (4-20) will all vanish except when m=p or when θ=0 or π. Thus

$$F_m(\theta_j) = \int_0^{\pi} E(\theta_j,\phi)\varepsilon^{-im\beta d_x \sin\theta_j \cos\phi} \sin\phi \, d\phi = 2 \sum_{n=-N}^{N} I_{mn}\varepsilon^{in\pi \cos\theta_j} . \quad (4\text{-}21)$$

From the above it immediately follows that

$$I_{mn} = \frac{1}{4\pi}\int_0^{\pi} F_m(\theta)\varepsilon^{-in\pi \cos\theta} \sin\theta \, d\theta \quad (4\text{-}22)$$

or

$$I_{mn} = \frac{1}{4\pi}\int_0^{\pi} \varepsilon^{-in\pi \cos\theta} \sin\theta \, d\theta \int_0^{\pi} E(\theta,\phi)\varepsilon^{-im\beta d_x \sin\theta \cos\theta} \sin\theta \, d\phi \quad (4\text{-}23)$$

where as stated before the integration must be performed numerically.

Obviously for an accurate description of the far-field pattern J which is determined by N would be so large that d_x would encompass too many wavelengths to supply any significant information about the presence of obstacles.

Spiral Array

The spiral shown in Fig. 4-5 will be considered as a one-dimensional variation of the planar array. Its isotropic far-field pattern is

$$E(\theta,\phi) = \sum_{m=0}^{\infty} I_m \varepsilon^{i\beta a_m \sin\theta \cos(\phi-\phi_n)} \quad (4\text{-}24)$$

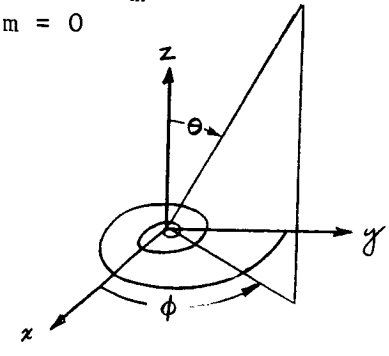

Fig. 4-5 Spiral Array Geometry

The above is made a function of θ alone by integrating to get

$$f(\theta) = \frac{1}{2\pi} \int_0^{2\pi} E(\theta,\phi)\varepsilon^{-i\phi} d\phi \qquad (4\text{-}25)$$

If the series (4-24) is valid, then

$$f(\theta) = \sum_{m=0}^{\infty} I_m J_1(\beta a_m \sin\theta)\varepsilon^{-i\phi_m} . \qquad (4\text{-}26)$$

Now the restriction is made that the radii $\{a_m\}$ constitute the roots of $J_1(\beta a_m) = 0$ for m=0,1,2,... . Then making use of the Bessel function orthogonality relation

$$\int_0^{\pi/2} J_1(\beta a_m \sin\theta)\, J_1(\beta a_n \sin\theta) \sin\theta \cos\theta \, d\theta = \begin{cases} \frac{1}{2} J_2^2(\beta a_n) & \text{for } m=n \\ 0 & m \neq n \end{cases} , \qquad (4\text{-}27)$$

the desired solution for I_m is found to be

$$I_m = \frac{2}{J_2^2(\beta a_m)} e^{i\phi_m} \int_0^{\pi/2} f(\theta) J_1(\beta a_m \sin\theta) \sin\theta \cos\theta \, d\theta . \qquad (4\text{-}28)$$

Even though this method offers the solution to a class of spiral array synthesis problems, it lacks the qualities necessary for two-dimensional obstacle location. The reason for this stems from the observation that the roots of $J_1(\beta a_m) = 0$ make the incremental radial spacing $\Delta a \approx \frac{1}{2}\lambda$. This in itself does not seem stringent until one notes that for $\Delta\phi$ small, the total radial jump at a particular angle ϕ_j (due to one encirclement) would be a sizable number of wavelengths. Going to large $\Delta\phi$ ($\Delta\phi \longrightarrow \pi$) remedies this difficulty but results in poor angular coverage. In either case the element positioning is too sparse to allow for good obstacle location.

Cylindrical Source Geometry

The geometry of a cylinder best suits the objectives of obstacle location on the Saturn booster and for that matter on most conventional rockets. Fortunately, this problem is fairly well behaved, and the research done on this project has led to some very useful synthesis methods for cylindrical sources.

A cylindrical source of radius "a" is shown in Fig. 4-6 where a source point is designated (a,ϕ',z') in cylindrical coordinates. The isotropic far-field expression for a continuous distribution is given by

$$E_c(\theta,\phi) = \int_{-\infty}^{\infty} \int_{-\pi}^{\pi} I(z',\phi')\varepsilon^{i\beta z' \cos\theta + i\beta a \sin\theta \cos[\phi-\phi']} d\phi' \, dz' \qquad (4\text{-}29)$$

and for discrete sources by

$$E_d(\theta,\phi) = \sum_{m=0}^{M} \sum_{n=-\infty}^{\infty} I_{mn}\varepsilon^{i\beta d_z n \cos\theta + i\beta a \sin\theta \cos(\phi-\phi_m)} \qquad (4\text{-}30)$$

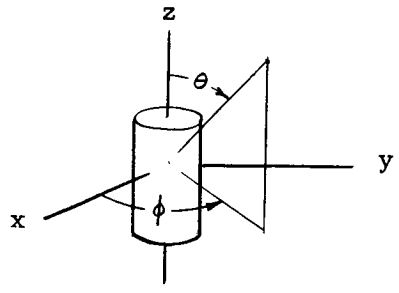

Fig. 4-6 Cylindrical Source

Woodward's Method Adapted for a Cylindrical Source

Here it will be assumed that the cylinder is of finite length L and that the current distribution $I(z',\phi')$ is continuous. For a physical problem the current is known to automatically fulfil these conditions. Then since the series for a continuous function is uniformly convergent[8] it is possible to approximate $I(z',\phi)$ by its finite Fourier series

$$I_a(z',\phi') = \sum_{-K}^{K}\sum_{-N}^{N} I_{nq}\varepsilon^{-iq\phi' - inz'\frac{2\pi}{L}}, |z'| < \frac{L}{2} \quad . \tag{4-31}$$

Using (4-31) in (4-29) and setting $I(z',\phi')=0$ for $|z'| > \frac{L}{2}$ gives

$$E_c(\theta,\phi) = 2\sum_{-K}^{K}\sum_{-N}^{N} I_{nq}\varepsilon^{-iq\phi} i^q J_q(\beta a \sin\theta) \frac{\sin\{(\beta\cos\theta - \frac{2\pi n}{L})\frac{L}{2}\}}{(\beta\cos\theta - \frac{2\pi n}{L})} \quad . \tag{4-32}$$

Calling upon the orthogonality relation

$$\frac{1}{2\pi}\int_{-\pi}^{\pi} \varepsilon^{im\phi - ik\phi} d\phi = \begin{matrix} 0 & m\neq k \\ 1 & m=k \end{matrix} \tag{4-33}$$

the double summation is reduced to a single summation by evaluating

$$F_q(\theta) \triangleq \frac{1}{2\pi}\int_{-\pi}^{\pi} E(\theta,\phi)\varepsilon^{iq\phi} d\phi \quad . \tag{4-34}$$

Left is

$$F_q(\theta) = 2\sum_{-N}^{N} I_{nq} i^q J_q(\beta a \sin\theta) \frac{\sin\{(\beta\cos\theta - \frac{2\pi n}{L})\frac{L}{2}\}}{(\beta\cos\theta - \frac{2\pi n}{L})} \quad . \tag{4-35}$$

Choosing the points θ_j such that

$$\cos\theta_p = \frac{P}{L} \quad p = 0, \pm 1, \pm 2, \ldots, \pm [L]$$

(the brackets $[L]$ denote the greatest integer in L) makes the argument of the sine term in equation (4-35)

$$\frac{L}{2}\left[\beta\cos\theta_p - \frac{2\pi n}{L}\right] = L\pi\left[\frac{p}{L} - \frac{n}{L}\right] = \pi(p-n) \quad .$$

In which case for $\theta = \theta_p$ all terms in the summation (4-35) are zero except the p^{th}. It therefore follows for $J_q(\beta a \sin\theta_n) \neq 0$

$$I_{nq} = \frac{F_q(\theta_n)}{i^q L J_q(\beta a \sin\theta_n)} = \frac{1}{2\pi i^q L J_q(\beta a \sin\theta_n)} \int_{-\pi}^{\pi} E(\theta_n,\phi) e^{iq\phi} d\phi \quad (4\text{-}36)$$

With regard to the above method the following comments are in order: (1) a good choice for the cylinder length L is L=N wavelengths where N is an integer, (2) care must be taken so that $J_q(\beta a \sin\theta_n) \neq 0$ for all values of n and q to be used, and (3) the limits N and K must be large enough to minimize the Gibb's phenomenon for current distributions likely to change abruptily (the reader is referred to the discussion of the problem of resolution found on page 57).

Woodward's method is superb for solution of continuous source function problems. However, let it again be stressed that for obstacle location with a dominant current concentrated in a relatively small spacial area, it is nearly always necessary to make the limits N and K extremely large in order to insure suitable convergence of the truncated series (4-31) near such sharp peaks. Another method was developed, however, which essentially solves the discrete problem posed by equation (4-30), and in this respect may find better application to obstacle location.

D-M Cylindrical Synthesis for Discrete Array

As inferred from the previous paragraph this method is highly recommended for the discrete cylindrical source problem. It does, however, involve an approximation, but by selecting a maximum error tolerance it is easy to establish a minimum allowable source radius which will guarantee that the error will never exceed the specified limit. As will be emphasized below, this error will be almost negligible for many practical cases.

The key to the ensuing work is an integral found in Magnus and Oberhettinger[9]

$$\int_0^{\pi/2} J_\mu(z\sin\theta)\, J_\nu(y\cos\theta)\, \sin^{\mu+1}\theta\, \cos^{\nu+1}\theta\, d\theta = \frac{z^\mu y^\nu J_{\mu+\nu+1}\left[\sqrt{z^2+y^2}\right]}{\left[z^2+y^2\right]^{(\mu+\nu+1)/2}} \qquad (4\text{-}37)$$

$$\nu > -1$$

$$\mu > -1$$

Also stated at this time are several other formulae dealing with Bessel functions which are about to be needed, namely,

$$J_0(z) = \frac{1}{2\pi}\int_0^{2\pi} \varepsilon^{iz\cos\theta}\, d\theta \qquad (4\text{-}38)$$

$$J_{\frac{1}{2}}(z) = \frac{\sin(z)}{\sqrt{\frac{\pi}{2}z}} \qquad (4\text{-}39)$$

$$J_{-\frac{1}{2}}(z) = \frac{\cos(z)}{\sqrt{\frac{\pi}{2}z}} \qquad (4\text{-}40)$$

For continuity in the following derivation let equation (4-30) for discrete sources on a cylinder of radius "a" with $d_z = \frac{\lambda}{2}$ be restated

$$E(\theta,\phi) = \sum_{-N}^{N}\sum_{0}^{M} I_{mn}\varepsilon^{in\pi\cos\theta + i\beta a\sin\theta\cos(\phi-\phi_m)} \qquad (4\text{-}30')$$

To start the solution one first defines the quantity

$$F_p(\theta) = \frac{1}{2\pi}\int_0^{2\pi} E(\theta,\phi)\varepsilon^{-i\beta a\sin\theta\cos(\phi-\phi_p)}\, d\phi \qquad (4\text{-}41)$$

On substituting the series (4-30) for $E(\theta,\phi)$ and using the trigonometric identity

$$\cos(\phi-\phi_m)-\cos(\phi-\phi_p) = 2\sin\frac{\phi_m-\phi_p}{2}\cos(\phi-\delta_{mp}) \qquad (4\text{-}42)$$

one gets

$$F_p(\theta) = \frac{1}{2\pi}\int_0^{2\pi}\sum\sum I_{mn}\varepsilon^{in\pi\cos\theta + i\beta a\sin\theta\, 2\sin\frac{\phi_m-\phi_p}{2}\cos(\phi-\delta)}\, d\phi$$

which according to (4-38) is

$$F_p(\theta) = \sum_{-N}^{N} \sum_{0}^{M} I_{mn} \varepsilon^{in\pi \cos\theta} J_o\{2\beta a \sin\theta \sin\left(\frac{\phi_n - \phi_p}{2}\right)\} \quad (4\text{-}43)$$

In an attempt to put the above solely in terms of Bessel functions let

$$G_{pq}(\theta) = F_p(\theta)\varepsilon^{-iq\pi \cos\theta} + F_p(\pi-\theta)\varepsilon^{+iq\pi \cos\theta} \quad (4\text{-}44)$$

$$= 2\sum_{-N}^{N} \sum_{0}^{M} I_{mn} \cos\{(n-q)\pi \cos\theta\} J_o\{2\beta a \sin\theta \sin \frac{\phi_m - \phi_p}{2}\} \quad (4\text{-}45)$$

From equation (4-40)

$$\cos\{(n-q)\pi \cos\theta\} = J_{-\frac{1}{2}}\{(n-q)\pi \cos\theta\}\sqrt{\frac{\pi}{2}(n-q)\pi \cos\theta}$$

and thus

$$G_{pq}(\theta) = 2\sum_{-N}^{N} \sum_{0}^{M} I_{mn} \sqrt{\frac{(n-q)\cos\theta}{2}}\, \pi J_{-\frac{1}{2}}\{(n-q)\pi\cos\theta\} J_o\{2\beta a \sin\theta \sin \frac{\phi_m - \phi_p}{2}\}. \quad (4\text{-}46)$$

Now consider the special form of (4-37) with $\mu=0$ and $v=-\frac{1}{2}$

$$\int_o^{\pi/2} J_o(z\sin\theta) \cos(y\cos\theta) \sin\theta d\theta = \int_o^{\pi/2} J_o(z\sin\theta) J_{-\frac{1}{2}}(y\cos\theta)\sqrt{\frac{\pi}{2}y\cos\theta} \sin\theta d\theta$$

$$= \sqrt{\frac{\pi}{2}} \frac{J_{\frac{1}{2}}(\sqrt{z^2+y^2})}{(z^2+y^2)^{\frac{1}{4}}} \quad (4\text{-}47)$$

which by (4-39) simplifies to

$$\int_o^{\pi/2} J_0(z \sin\theta) \cos(y \cos\theta) \sin\theta \, d\theta = \frac{\sin(\sqrt{z^2+y^2})}{\sqrt{z^2+y^2}}. \quad (4\text{-}48)$$

Now returning to the expression for $G_{pq}(\theta)$ and making use of the above it

is seen that

$$\int_0^{\pi/2} G_{pq}(\theta)\sin\theta\, d\theta = 2\sum_{-N}^{N}\sum_{0}^{M} I_{mn} \frac{\sin\left\{\sqrt{\left(2\beta a \sin\frac{\phi_m-\phi_p}{2}\right)^2 + (n-q)^2\pi^2}\right\}}{\sqrt{\quad}}$$

$$= 2\sum_{-N}^{N}\sum_{0}^{M} I_{mn} \frac{\sin\left\{\pi\sqrt{\left(4a \sin\left(\frac{\phi_m-\phi_p}{2}\right)\right)^2 + (n-q)^2}\right\}}{\pi\sqrt{\left(4a \sin\frac{\phi_m-\phi_p}{2}\right)^2 + (n-q)^2}}. \quad (4\text{-}49)$$

It is equation (4-49) which is capable of yielding the desired solution. As will be shown, this objective will be achieved at a sacrifice of generality in the problem by requiring the source to have a sufficiently large source radius to guarantee a selectable error figure.

Consider the expansion

$$\sqrt{A^2+B^2} = A+\frac{1}{2}A^{-1}B^2+\frac{1}{2}\left(-\frac{1}{2}\right)\frac{A^{-3}B^4}{2!} + \cdots = A\sum_{k=0}^{\infty}\frac{(-1)^k\left(-\frac{1}{2}\right)_k}{k!}\left(\frac{B^2}{A^2}\right)^k \quad (4\text{-}50)$$

where $(a)_k = (a)(a+1)(a+2)\ldots(a+k-1)$

$(a)_0 = 1$

Denoting

$Q = (n-q)$

$\Delta = \phi_m - \phi_p$

it is desired to choose the radius "a" appearing in the square root in equation (4-49) such that

$$\sqrt{(4a \sin(\Delta/2))^2 + Q^2} \approx \begin{cases} 4a\sin(\Delta/2) & \text{for } \Delta\neq 0 \\ Q & \text{for } \Delta = 0 \end{cases}. \quad (4\text{-}51)$$

When B<A the expansion (4-50) is an absolutely convergent alternating series, and thus, by a well known theorem concerning such a series, the

error in truncating the series is less than the magnitude of the first term omitted.[10] For the choice

$$B=0.1A$$

$$\sqrt{A^2+B^2} = A+\frac{1}{2}(.01)A+.... = A(1.00000+ .005+ ...)$$

implies $\sqrt{A^2+B^2} \approx A$ with a maximum error of 0.5%.

Similarly for

$$B=0.05A$$

$$\sqrt{A^2+B^2} = A(1.0000+ \frac{1}{2} .0025 + ...)$$

$$\approx A \text{ with a maximum error of } 0.125\%.$$

It should be made clear that the error of concern expresses the maximum percentage of an actually occurring source element that can be falsely detected at another source location. Needless to say, the above indicates that for the choice $\alpha \leq .1$ in $B=\alpha A$ such error will normally be smaller than the error introduced by a digital computer using numerical integration to find the unknown coefficients. Examination of the reconstruction series (4-30) further suggests that the approximation error and the numerical integration error both constitute insignificant "hash" relative to the elements actually producing and distorting the pattern in obstacle location.

Now to determine "a" let $\{\phi_j\}$ be carefully chosen to make

$$\sin(\frac{\phi_m-\phi_p}{2}) = \frac{m-p}{J} . \qquad (4\text{-}52)$$

Deeming that the following can be better illustrated by a numerical example assume $\alpha=0.1$ fixes an adequate error bound. Then "a" must be chosen so that

$$Q_{max} = \left|(n-q)_{max}\right| = 0.1\left|4a \sin(\Delta_{minimum}/2)\right| \qquad (4\text{-}53)$$

where

$$\sin\left[\frac{\Delta_{min}}{2}\right] = \frac{1}{J} .$$

Solving (4-53) gives

$$a = \frac{10\ \left|(n-q)_{max}\right|}{4\frac{1}{J}} = 2.5\ J\ \left|(n-q)_{max}\right| \quad \text{wavelengths} .$$

Thus for a maximum theoretical error of 0.5%, the selection

$$a = 2.5\ J\ \left|(n-q)_{max}\right| = \text{minimum cylindrical radius} \qquad (4\text{-}54)$$

enables one to determine the array elements in

$$E(\theta,\phi) = \sum_{-N}^{N}\sum_{0}^{M} I_{mn}\varepsilon^{in\pi\cos\theta + i\beta a\sin\theta\cos(\phi-\phi_m)} \qquad (4\text{-}30)$$

by the integral

$$I_{mn} = \frac{1}{2}\int_{o}^{\pi/2} G_{mn}(\theta)\sin\theta d\theta = \frac{1}{2}\int_{o}^{\pi/2}\left\{ F_m(\theta)\varepsilon^{-in\pi\cos\theta} + F_m(\pi-\theta)\varepsilon^{+in\pi\cos\theta}\right\}\sin\theta d\theta \qquad (4\text{-}55)$$

where

$$F_m(\theta) = \frac{1}{2\pi}\int_{o}^{2\pi} E(\theta,\phi)\varepsilon^{-i\beta a\sin\theta\cos(\phi-\phi_m)} d\phi . \qquad (4\text{-}41)$$

There are several other methods for cylindrical synthesis which may be of some interest and will be included in this report.

Small Cylinder Radius ($\beta a<2.3$), Reduced Matrix

For $\beta a<2.3$ it is possible to employ the altered matrix method introduced on page 38 for the circular array. With discrete sources spaced $d_z = \frac{\lambda}{2}$ the cylindrical pattern is

$$E(\theta,\phi) = \sum_{-N}^{N} \sum_{0}^{M} I_{mn} e^{in\pi \cos\theta + i\beta a \sin\theta \cos(\phi-\phi_m)} \qquad (4\text{-}30')$$

Evaluation of

$$H_p(\theta) = \frac{1}{2\pi} \int_0^{2\pi} E(\theta,\phi) e^{-ip\phi} \, d\phi \qquad (4\text{-}56)$$

using the above expansion (4-30') for $E(\theta,\phi)$ gives

$$H_p(\theta) = \sum_{-N}^{N} \sum_{0}^{M} I_{mn} e^{in\pi \cos\theta} \, i^p \, J_p(\beta a \sin\theta) \, e^{-ip\phi_m} \qquad (4\text{-}57)$$

Now consider

$$C_{pn} \triangleq \int_0^{\pi} \frac{H_p(\theta) \, e^{-in\pi \cos\theta} \sin\theta}{i^p \, J_p(\beta a \sin\theta)} \, d\theta \qquad (4\text{-}58)$$

The condition $\beta a<2.3$ restricts the argument of $J_p(\beta a \sin\theta)$ so that the function has no zeros except at $\theta = 0$ and π ($p>0$). Then since the numerator in the integrand of (4-58) has a $\sin\theta$ term, by L'Hospital's rule it is obvious that the said integrand has no singularities due to the zeros of $J_p(\beta a \sin\theta)$, and hence C_{pn} will always exist for physically obtainable patterns (no singularities). The fact is that the matrix variation to be used in this section can also be extended to larger radii cylinders provided the condition $H_p(\theta)e^{in\pi \cos\theta}$ be odd about $\theta=\frac{\pi}{2}$ is satisfied in the range $(0,\pi)$. Under such circumstances the first order singularities due to $J_p(\,)$ would cancel and thereby enable C_{pn} to exist as a Cauchy principal value.

Now whenever C_{pn} meets its existence conditions, the system of equations generated by

$$C_{pn} = \int_0^{\pi} \frac{H_p(\theta)\varepsilon^{-in\pi\cos\theta}\sin\theta\, d\theta}{i^p J_p(\beta a \sin\theta)} = \sum_0^M I_{mn}\varepsilon^{-imp(\Delta)} \qquad (4\text{-}60)$$

can be solved for the unknowns I_{mn}. The above has the same coefficient matrix that yielded the great simplification for the circular array. This time

$$\begin{bmatrix} C_{n,-N} \\ \vdots \\ C_{n,-1} \\ C_{n,0} \\ C_{n,1} \\ \vdots \\ C_{n,N} \end{bmatrix} = \begin{bmatrix} 1 & \varepsilon^{iN\Delta} & & \varepsilon^{iMN\Delta} \\ \vdots & & & \\ 1 & \varepsilon^{i\Delta} & \varepsilon^{2i\Delta} & \varepsilon^{iM\Delta} \\ 1 & 1 & 1 \ldots & 1 \\ 1 & \varepsilon^{-i\Delta} & & \varepsilon^{-iM\Delta} \\ \vdots & & & \\ 1 & \varepsilon^{-iN\Delta} & & \varepsilon^{-iMN\Delta} \end{bmatrix} \begin{bmatrix} I_{0n} \\ I_{1n} \\ I_{2n} \\ \vdots \\ I_{Mn} \end{bmatrix} \qquad (4\text{-}62)$$

where $M=2N$ and $n=0,\pm1,\pm2,\ldots,\pm N$. But the above gives an unexpected bonus in that the $(M+1)^2$ unknowns can be solved for $(M+1)$ at a time. Created is a terrific time and space savings in a digital computer solution for there is only one coefficient matrix to be successively reused with each different column ($C_{n,j}$) and it is one whose reduced form is already known (see page 42). The importance of the size of this matrix is more important than one might think because a matrix with $(M+1)^2$ terms usually presents no storage problem whereas a matrix with $(M+1)^4$ elements (as occurs for a general two-dimensional problem) could easily exceed the core storage limits on many present-day computers.

Ksienski Approximation Extended to Cylindrical Sources

The final technique to be examined is an extension to the cylindrical

array of the Ksienski approximation already discussed in connection with the circular array. A digital computer program has been written for this method, and some of the results of this program are presented in Chapter V.

Restating the isotropic field for a cylindrical array of radius "a" with $d_z = \frac{1}{2}\lambda$

$$E(\theta,\phi) = \sum_{m=o}^{M} \sum_{-N}^{N} I_{mn} \varepsilon^{in\pi \cos\theta + i\beta a \sin\theta \cos(\phi-\phi_m)} \qquad (4\text{-}30')$$

Then

$$G_p(\theta) = \frac{1}{2\pi} \int_0^{2\pi} E(\theta,\phi) \varepsilon^{-i\beta a \sin\theta \cos(\phi-\phi_p)} d\phi \qquad (4\text{-}62)$$

$$= \sum_{0}^{M} \sum_{-N}^{N} I_{mn} \varepsilon^{in\pi \cos\theta} J_o\{2\beta a \sin\theta \sin(\frac{\phi_m - \phi_p}{2})\}$$

Oddly enough here is a method which will work for numerical integration, but not for the exact process. For if data points θ_k are determined according to

$$\sin\theta_k = \frac{k}{K} \qquad (0,\pi/2)$$

$$1 - \frac{k}{K} \qquad (\pi/2,\pi)$$

with the points 0 and π excluded,

and if the array points are properly chosen so that

$\sin \frac{\phi_m - \phi_p}{2} = (m-p)/J$, a radius "a" can be found which will make the argument $x=2\beta a \sin\theta \sin\frac{\phi_m - \phi_p}{2}$ best approximate the roots of $J_0(x)=0$. No optimum choice has been found, but scrutiny of a table of zero-order Bessel functions suggests

$2\beta a \frac{1}{K} \frac{}{J} = 2.9$ or 5.8 as convenient selections. As before a maximum error of about 22% or 10% respectively is hard to avoid, and thus

the D-M approximation stated previously is much superior.

CHAPTER V

APPLICATION TO RADIATION PATTERNS

In this chapter some of the synthesis methods discussed in Chapters II, III and IV are applied to radiation patterns which are (1) measured with a known antenna and obstacles, or (2) calculated from a known set of sources. An object is to demonstrate that the methods of obstacle location developed in this report can be applied to a measured amplitude pattern to yield a knowledge of obstacles located in the vicinity of an antenna. Another object is to determine the relative ease of using the various methods and the accuracy with which they give the correct source distribution. The second process, in which a pattern is calculated from a known set of sources and then used in our obstacle-location procedure to redetermine the original set of sources, is not as dramatic as the first but just as effective. It is used when measured patterns for a particular source geometry are not available.

Fourier Series for Linear Array

Measured antenna patterns at 8 Gc, with a rectangular aperture at the center of a square plane 4 feet on a side, have been analyzed by the one-dimensional Fourier series discussed previously to determine if various obstacles and plane distortions would affect the synthesized array currents as predicted and could thus be located. The sides of the slot were parallel to those of the ground plane. The pattern plane was chosen as the E-plane of the aperture antenna, perpendicular to the ground plane and to the long side of the aperture. The receiving antenna was sensitive only to polarization in the pattern plane.

Structures 3 in. long, 2.5 in. high, and 2.5 in. thick at the base, formed by bending a conducting sheet, were attached successively at diffe-

rent positions on the ground plane. In addition the ground plane was bent sharply for some measurements. The resulting patterns were studied in an attempt to locate the structures and the bend from the pattern alone.

An array spacing of $\lambda/2$ was chosen and the patterns over 180° were synthesized. In some cases a difference array was formulated, using the calculated pattern of the aperture on an infinite ground plane as a standard; in other cases the synthesized array for the distorted pattern was treated directly.

Figure 5-1(a) is the measured power pattern obtained by bending the ground plane sharply upward at 45° at a distance of 6.75 in. from the aperture center. The bend is parallel to a long side of the slot and transverse to the pattern plane. The pattern is greatly distorted from the ideal and is asymmetrical.

In Fig. 5-1(b) the plot of relative synthesized array currents is shown for an array assumed to lie in the pattern plane and on the plane ground surface (before bending). Since the geometry differs greatly from that of an infinite ground plane the difference array currents are not shown, but in fact do not differ significantly in appearance from the spectrum shown. The positions of the bend, the edge, and bend plus edge are shown. It is seen that the spectrum plot brings out the bend position and relative importance very clearly. The greatest field contributions seem to be from sources lying to the right of the known bend position; that is, farther from the aperture. This indicates that in the physical problem the greatest field distorting contributions are reflections from the bent-upward ground plane close to the bend, rather than from the bend itself.

On this plot the edge of the ground plane is not shown clearly, and

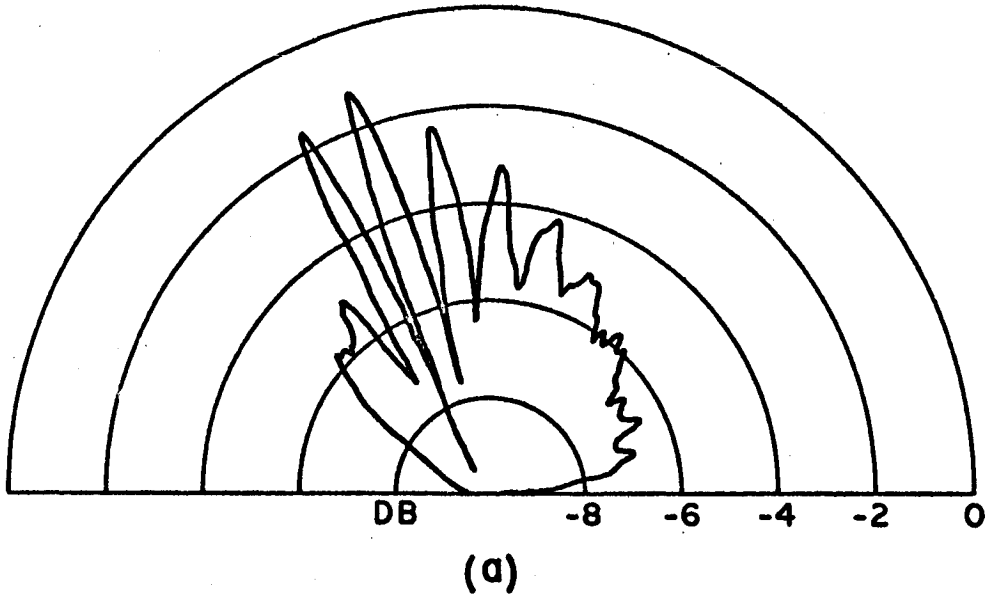

(a)

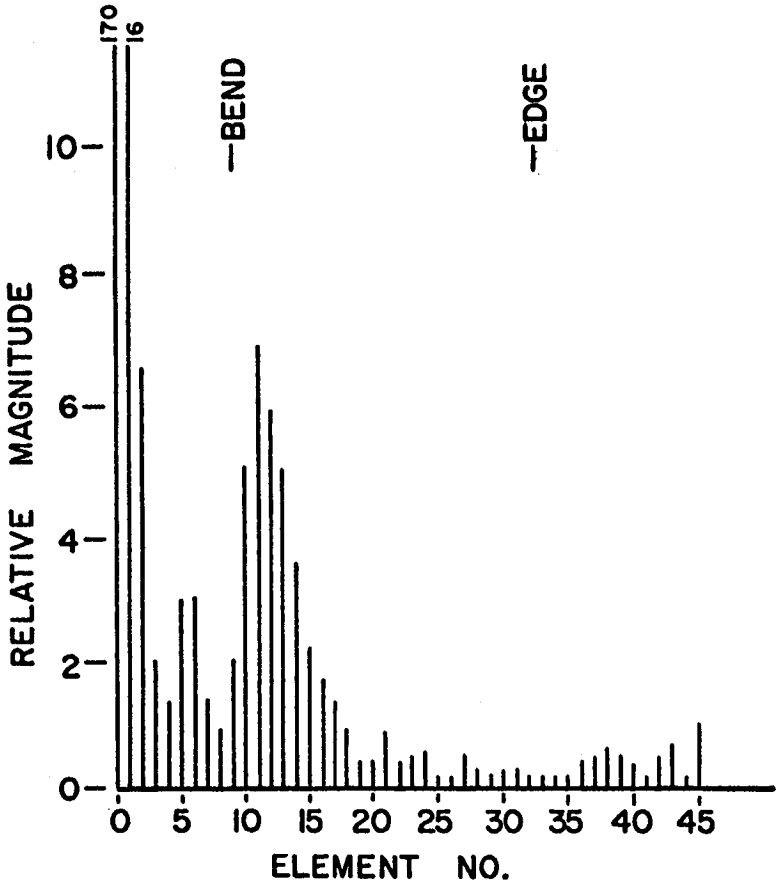

(b)

Fig. 5-1. Pattern and Spectrum for Bend on Finite Ground Plane

a spurious current at a distance equal to edge plus bend distance is also indefinite.

Figures 5-2(a) and (b) are the pattern and spectrum plots for the same bent ground plane with one of the conducting structures placed on the ground plane and in the pattern plane. It is 4 in. from the aperture and on the opposite side of the aperture from the bend. Both the obstacle at 4 in. and the bend are shown clearly, with the bend contributions again lying outside the actual position of the bend. A spurious indication should appear at bend plus obstacle distances, and this does appear although not as clearly as the true indications. The edge indications are again negligible, but spurious responses at edge plus obstacle distances and edge plus bend distances have definite values.

In Figs. 5-3(a) and (b) appear the pattern and spectrum plot for the flat ground plane with two conducting obstacles. Both are in the pattern plane, one 6 in. from the aperture and one 8 in. on the opposite side of the aperture. Both are easily distinguishable on the spectrum despite the fact that on the plot they appear to be separated by 2 in. which is smaller than any one of their physical dimensions. When the edges are considered many spurious responses should appear in this spectrum, but these are seen to be negligibly small.

Figures 5-4(a) and (b) illustrate the effect of a structure not in the pattern plane and thus off the array axis. They are for the flat ground plane with one conducting obstacle placed 12 in. down the line of the array and 6 in. off the line. A smaller aperture was used for this pattern, but otherwise all conditions were the same. Fig. 5-4(b) is the spectrum of currents for the difference array. Subtracted from the array for the distorted pattern was that for the aperture on an infinite ground

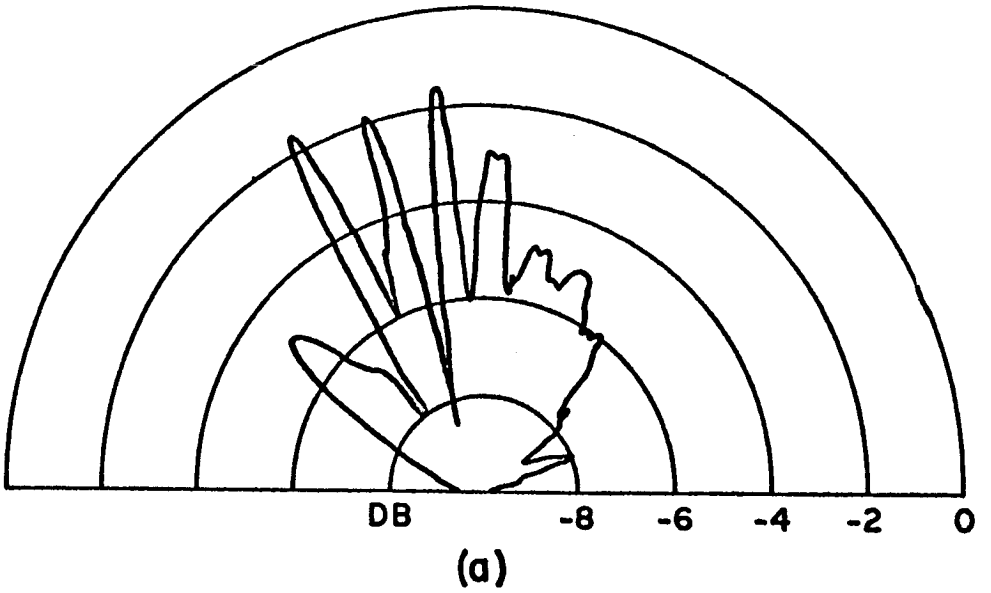

(a)

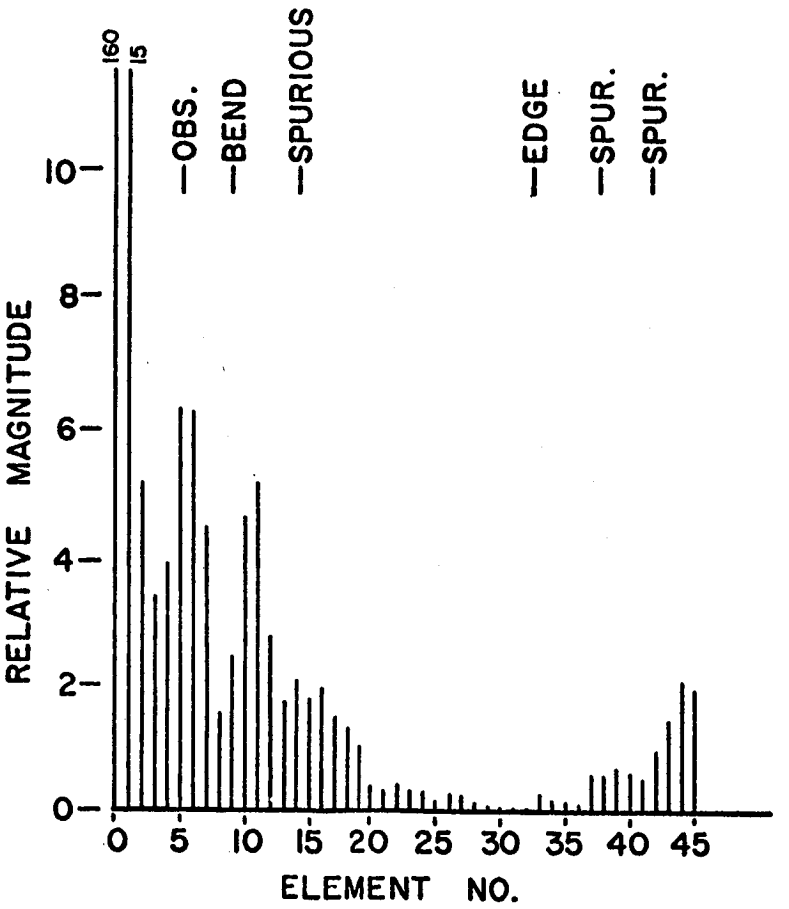

(b)

Fig. 5-2. Pattern and Spectrum for Bend and Obstacle on Finite Ground Plane

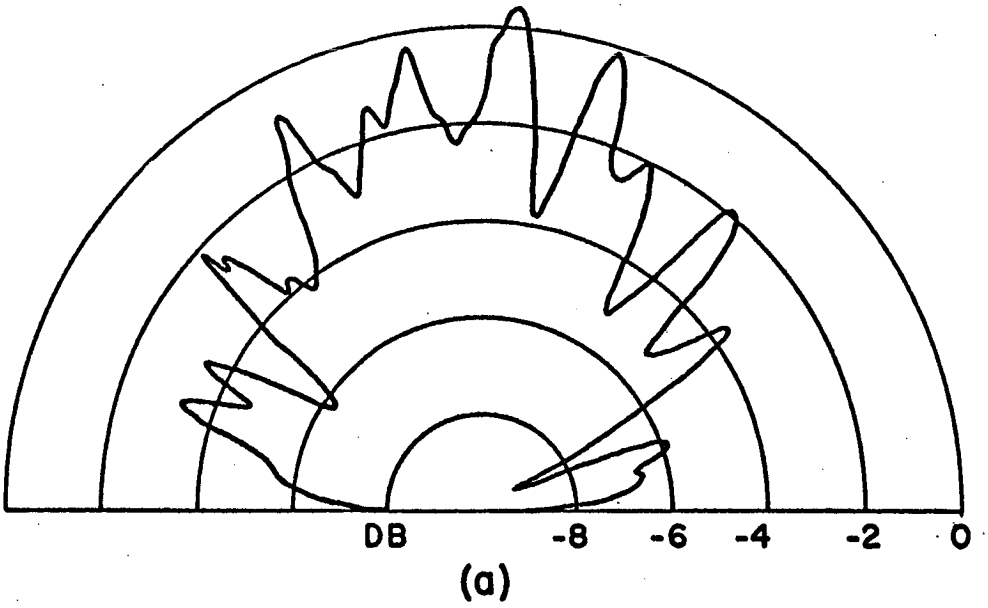

(a)

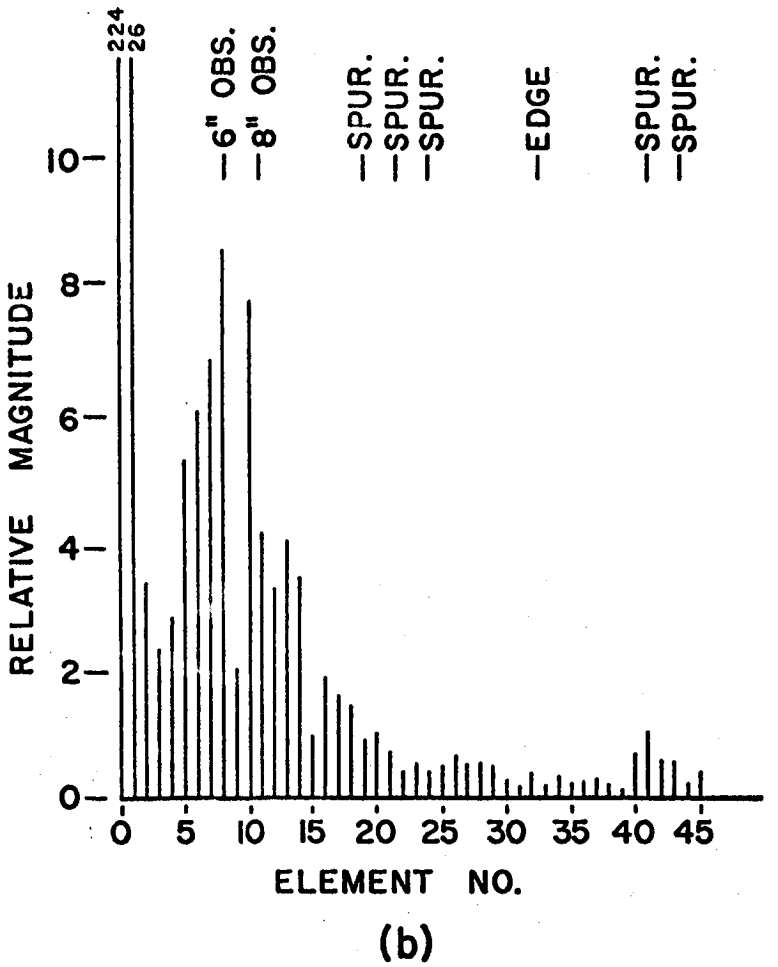

(b)

Fig. 5-3. Pattern and Spectrum for Two Obstacles on Finite Ground Plane

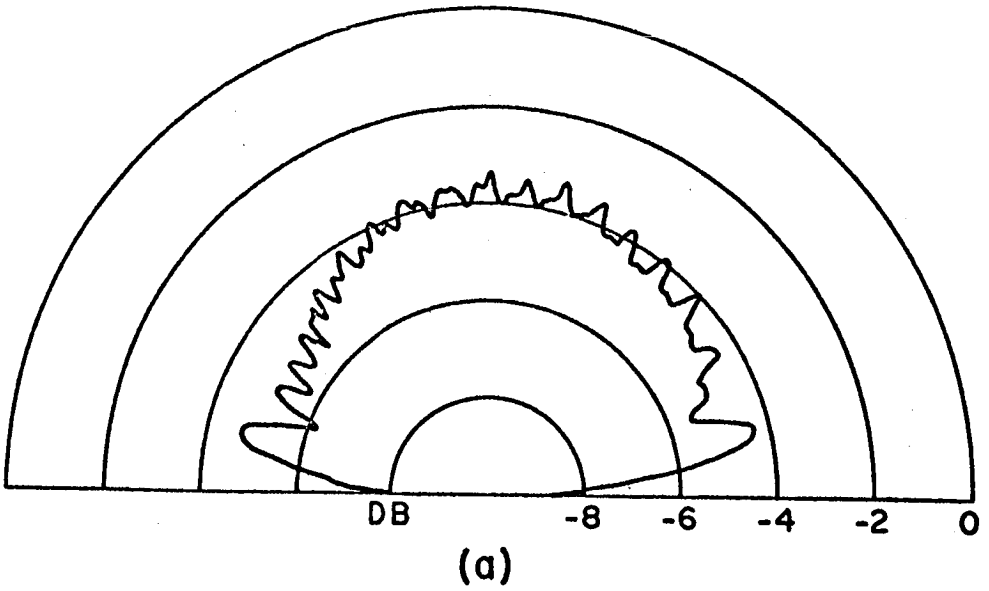

(a)

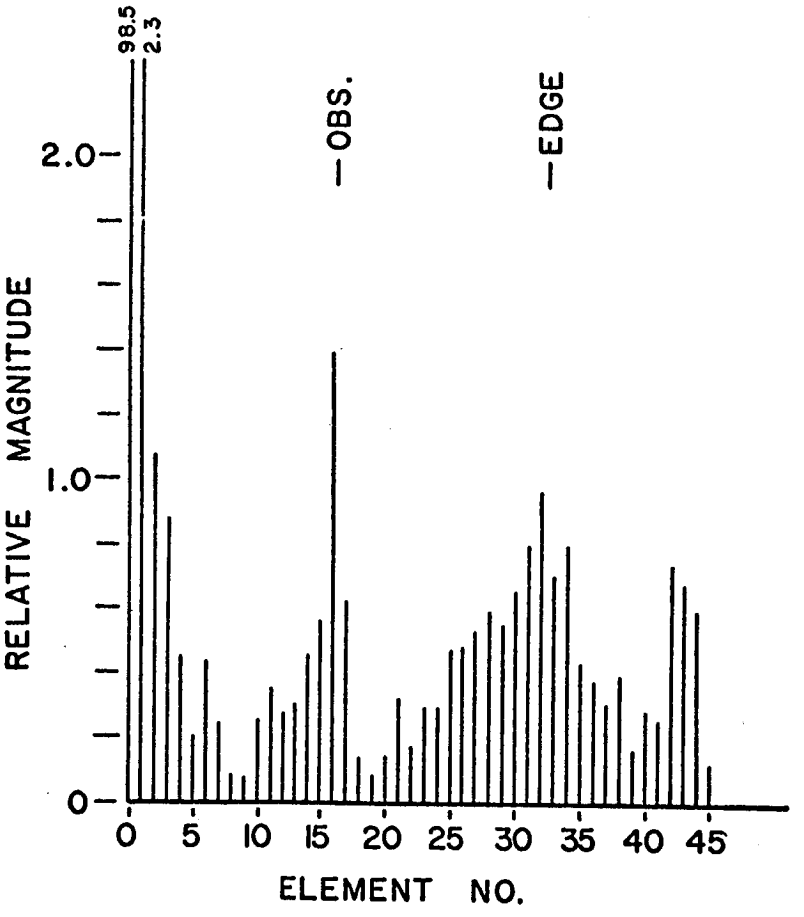

(b)

Fig. 5-4. Pattern and Difference Spectrum for off-Axis Obstacle

plane. The obstacle shows up well on this plot, and so do the edges of the ground plane. The indication near the end of the spectrum is apparently spurious corresponding to edge plus obstacle distances which lies just off the end of the plot. This example shows that objects off the array axis can be located approximately.

The interpretation was of course made simpler by choosing the pattern plane in relation to the known obstacle position. As stated previously it is necessary in general to examine many patterns, forming an array for each pattern, to locate all the distorting structures in the near-field.

Woodward Method for a Linear Source

Woodward's method has earlier been strongly recommended for the rectangular source synthesis problem. Recall that this method assumes a continuous source distribution of finite physical extent. It was also stressed at that time that a dominant central element typical of the obstacle location problem in many ways approximates a step discontinuity. FORTRAN programs have been written for both the linear and rectangular sources, but only the linear examples will be presented since they economize computer time while graphically illustrating the important behavioral characteristics of both geometries.

Presented in Fig. 5-5(a) is a discontinuous source function simulating a worst case obstacle location occurrence. The source is length L = 100 wavelengths containing two current pulses of different widths. The complex Fourier series used to synthesize the above from its far-field pattern was truncated to include 200 terms (see page 54). Fig. 5-5(b) shows the close resemblance between the regenerated source and the original. Figures 5-6(a) and 5-6(b) demonstrate the effect of narrowing one of the pulses to less than the Dirichlet bandwidth employed.

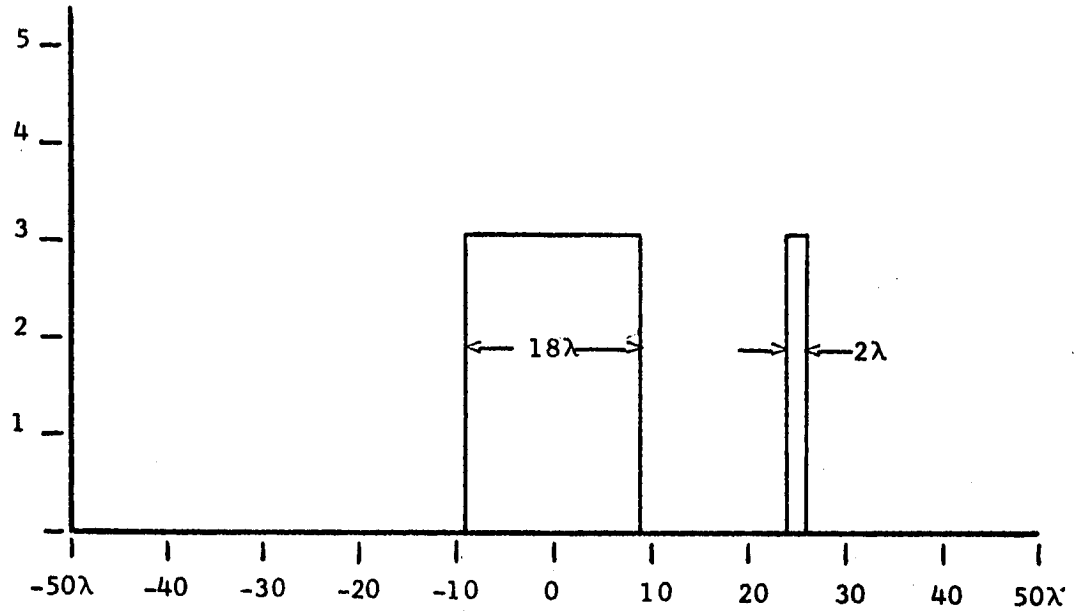

(a) Rectangular Current Pulses

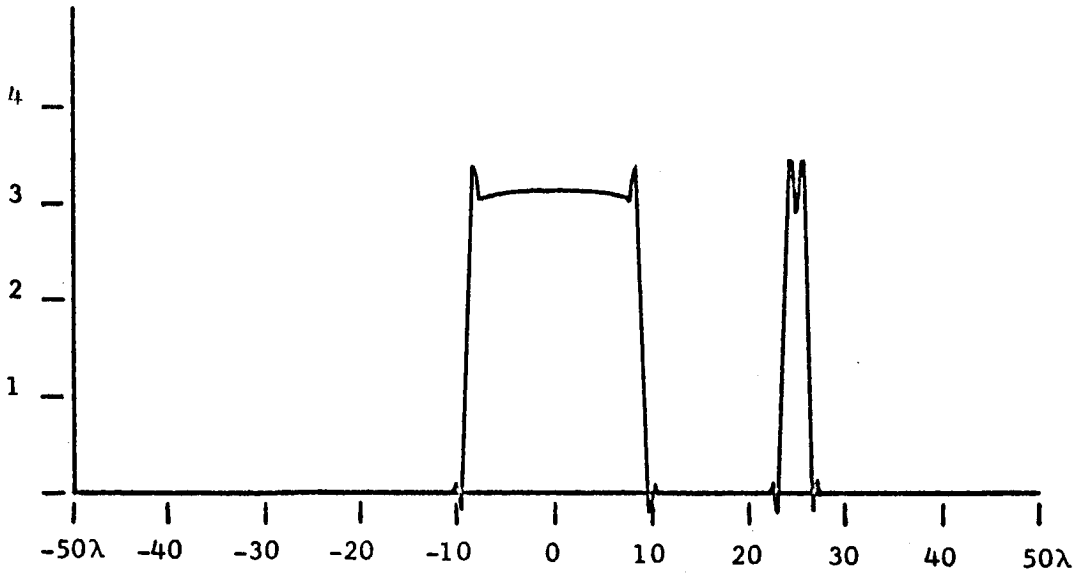

(b) Regenerated Distribution Using Woodward's Method

FIGURE 5-5

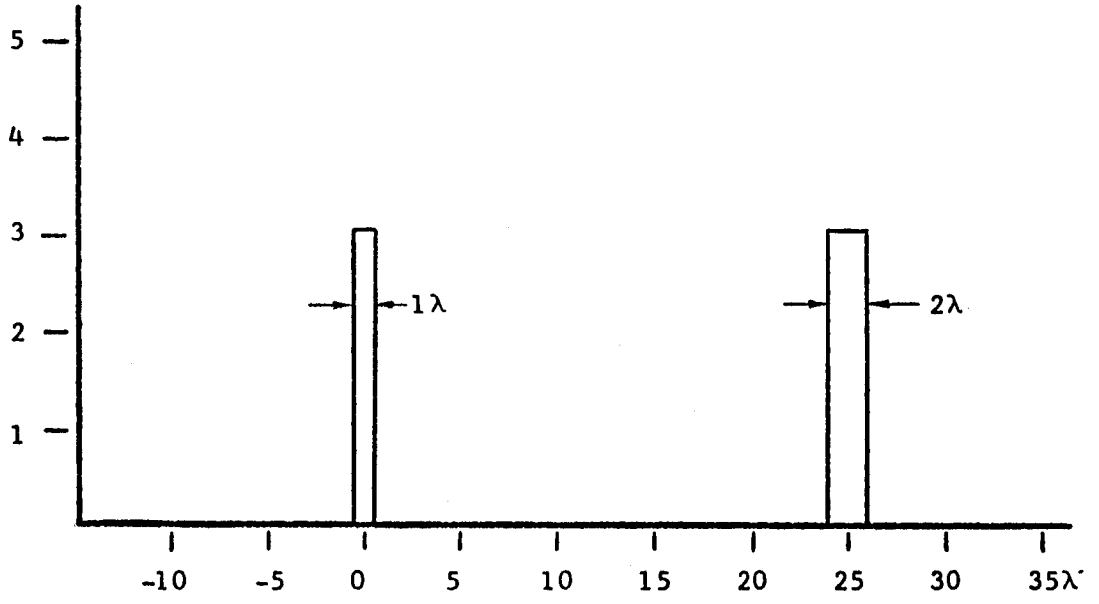

(a) Rectangular Current Pulses

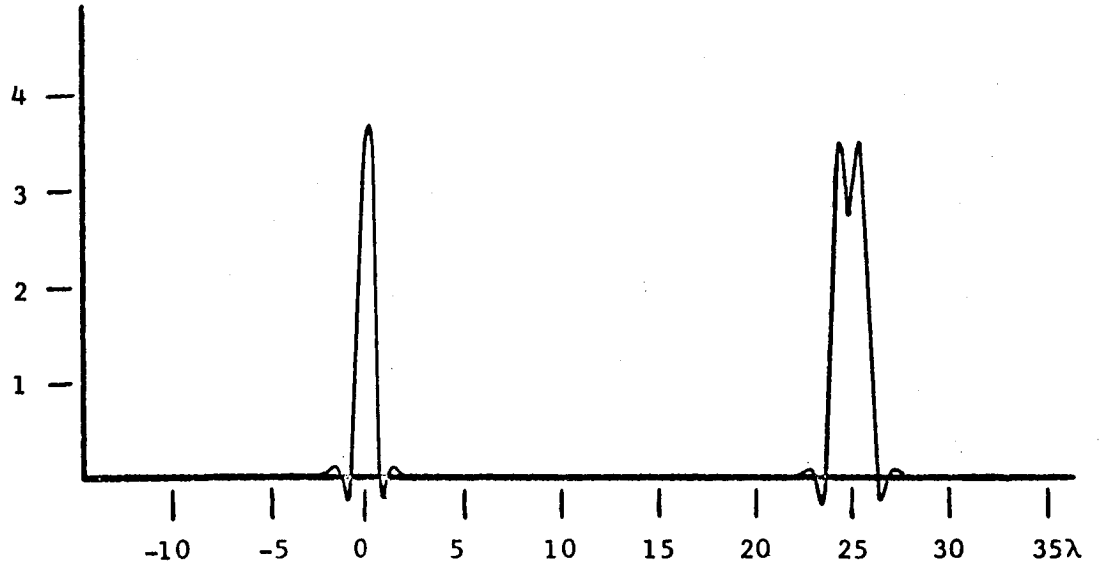

(b) Regenerated Distribution Using Woodward's Method

FIGURE 5-6

As can be seen, the pulse is still detected but now oscillates and peaks above the 9% optimum Gibb's error corresponding to the loss of resolution.

Ksienski Approximation for a Cylindrical Source

First observe that even though this method has been programmed, it is inferior to the D-M approximation described on page 63. In an attempt to minimize the error associated with this approach, it was programed to run with $\beta a=2.9JK$. For this value it was experimentally found hard to do better than the forecast error of 22% in the $J_0(x)$ approximation. However, part of the effect of this error is lost in the final integration with respect to θ since the maximum does not occur for all θ_j. Also the 22% error figure can be forced to appear in the terms connected with the elements adjacent to a true field producing source. This might destroy the regenerated field pattern produced by the synthesized array, but for obstacle location the general vicinity of a pattern disturbing source is still strongly indicated, spread out though it may be.

Listed in Table 5-1 are the magnitudes of the currents that this method would yield for the pattern

$$E(\theta,\phi) = 154\ \varepsilon^{i\beta a \sin\theta \cos\phi}$$

This is the far-field of the central element isolated by itself so that ideally all currents but I_{00} should be zero for exact synthesis. From Table 5-1 it is evident that the actual source is properly detected, nevertheless, non-existent elements with amplitudes up to about 4.4% of I_{00} affirm the presence of an inherent error which is too large to be attributed to numerical integration.

TABLE 5-1

m	n	I_{mn}
0	0	154.32
0	1	2.46
0	2	-2.07
0	3	1.72
0	4	-1.80
0	5	1.77
0	6	-1.70
0	7	1.77
0	8	-1.79
0	9	1.78
0	10	-1.86
0	11	1.88
0	12	-1.83
0	13	1.84
0	14	-1.82
0	15	1.99
1	0	5.95
1	1	5.79
1	2	5.56
1	3	-.09
1	4	-4.69
1	5	-2.57
1	6	4.89
1	7	-.11
1	8	-4.09
1	9	3.49
1	10	-.98
1	11	-.89
1	12	2.62
1	13	-3.49
1	14	3.30
1	15	-1.71
2	0	2.18
2	1	3.11
2	2	1.42
2	3	2.28
2	4	-.76
2	5	.01
2	6	-4.12
2	7	1.49
2	8	.06
2	9	4.83
2	10	-5.45
2	11	-.62
2	12	6.60
2	13	-2.74
2	14	-4.81
2	15	.67
3	0	-1.85
3	1	-.97
3	2	.10
3	3	1.12
3	4	-.63
3	5	5.15
3	6	-.38
3	7	.28
3	8	.00
3	9	-.04
3	10	-1.82
3	11	-.54
3	12	1.30
3	13	.43
3	14	1.28
3	15	1.82
4	0	3.34
4	1	-.93
4	2	-.55
4	3	3.14
4	4	1.29
4	5	-.05
4	6	1.41
4	7	-.60
4	8	1.68
4	9	-2.08
4	10	-2.43
4	11	.03
4	12	.23
4	13	1.93
4	14	-.18
4	15	.52
5	0	1.19
5	1	-.77
5	2	-3.52
5	3	.32
5	4	.68
5	5	-1.38
5	6	-1.84
5	7	-.04
5	8	-.73
5	9	3.30
5	10	1.46
5	11	1.45
5	12	-.63
5	13	-.67
5	14	-3.24
5	15	1.96
6	0	-1.31

m	n	I_{mn}
6	1	.86
6	2	3.70
6	3	1.14
6	4	-.66
6	5	-1.23
6	6	1.30
6	7	-2.07
6	8	2.13
6	9	-1.71
6	10	-.70
6	11	-1.26
6	12	.09
6	13	.46
6	14	-1.80
6	15	.95
7	0	3.15
7	1	-.34
7	2	3.61
7	3	-.68
7	4	1.50
7	5	-.68
7	6	2.30
7	7	1.41
7	8	-2.78
7	9	-.57
7	10	-3.06
7	11	-1.91
7	12	1.23
7	13	.80
7	14	2.02
7	15	1.49
8	0	3.00
8	1	-.83
8	2	3.71
8	3	-.37
8	4	.67
8	5	-.59
8	6	2.67
8	7	1.49
8	8	-3.05
8	9	-.05
8	10	-2.47
8	11	-1.84
8	12	.93
8	13	.61
8	14	1.96
8	15	1.55
9	0	-1.09
9	1	.89
9	2	3.76
9	3	.61
9	4	-1.20
9	5	-1.12
9	6	1.89
9	7	-1.95
9	8	1.51
9	9	-1.20
9	10	-.51
9	11	-.89
9	12	.83
9	13	.27
9	14	-1.37
9	15	.98
10	0	1.55
10	1	-1.29
10	2	-4.52
10	3	.37
10	4	-.07
10	5	-2.09
10	6	-2.24
10	7	-.55
10	8	-1.12
10	9	4.69
10	10	2.76
10	11	1.94
10	12	-.36
10	13	-2.00
10	14	-4.16
10	15	1.61
11	0	4.64
11	1	-.56
11	2	-.61
11	3	4.06
11	4	1.77
11	5	-.69
11	6	1.32
11	7	-.25
11	8	1.56
11	9	-2.35
11	10	-3.05
11	11	.14
11	12	.43
11	13	2.26
11	14	-.26
11	15	.03
12	0	-.53
12	1	-.68
12	2	.22
12	3	1.24
12	4	-1.69
12	5	5.73
12	6	-1.36

m	n	I_{mn}
12	7	.10
12	8	.07
12	9	-.32
12	10	-2.24
12	11	-.79
12	12	1.38
12	13	-.02
12	14	1.07
12	15	2.00
13	0	2.16
13	1	3.70
13	2	1.86
13	3	2.54
13	4	-.81
13	5	-.85
13	6	-3.80
13	7	1.57
13	8	-.43
13	9	5.35
13	10	-5.20
13	11	-1.01
13	12	6.77
13	13	-3.32
13	14	-4.31
13	15	.39
14	0	5.58
14	1	5.71
14	2	5.11
14	3	.43
14	4	-4.73
14	5	-2.81
14	6	3.92
14	7	.15
14	8	-4.34
14	9	3.55
14	10	-.79
14	11	-1.88
14	12	2.74
14	13	-4.00
14	14	3.20
14	15	-1.67
15	0	~~148.87~~ 1.49
15	1	1.23
15	2	-1.70
15	3	1.86
15	4	-1.64
15	5	1.44
15	6	-1.86
15	7	1.39
15	8	-1.82
15	9	1.71
15	10	-2.18
15	11	1.82
15	12	-1.98
15	13	1.55
15	14	-1.99
15	15	1.75
16	0	6.06
16	1	5.82
16	2	5.03
16	3	-.04
16	4	-4.81
16	5	-2.89
16	6	5.08
16	7	.48
16	8	-3.93
16	9	3.69
16	10	-.75
16	11	-.97
16	12	2.51
16	13	-3.04
16	14	3.62
16	15	-2.13
17	0	2.12
17	1	3.06
17	2	1.47
17	3	2.51
17	4	-.71
17	5	-.15
17	6	-4.23
17	7	1.49
17	8	-.00
17	9	4.77
17	10	-5.71
17	11	-.84
17	12	6.66
17	13	-2.77
17	14	-4.88
17	15	.74
18	0	-1.85
18	1	-.97
18	2	.10
18	3	1.12
18	4	-.63
18	5	5.15
18	6	-.38
18	7	.28
18	8	.00
18	9	-.04
18	10	-1.82
18	11	-.54
18	12	1.30

m	n	I_{mn}
18	13	.43
18	14	1.28
18	15	1.82
19	0	3.34
19	1	-.93
19	2	-.55
19	3	3.14
19	4	1.29
19	5	-.05
19	6	1.41
19	7	-.60
19	8	1.68
19	9	-2.08
19	10	-2.43
19	11	.03
19	12	.23
19	13	1.93
19	14	-.18
19	15	.52
20	0	1.19
20	1	-.77
20	2	-3.52
20	3	.32
20	4	.68
20	5	-1.38
20	6	-1.84
20	7	-.04
20	8	-.73
20	9	3.30
20	10	1.46
20	11	1.45
20	12	-.63
20	13	-.67
20	14	-3.24
20	15	1.96
21	0	-1.31
21	1	.86
21	2	3.70
21	3	1.14
21	4	-.66
21	5	-1.23
21	6	1.30
21	7	-2.07
21	8	2.13
21	9	-1.71
21	10	-.70
21	11	-1.26
21	12	.09
21	13	.46
21	14	-1.80
21	15	.95
22	0	3.15
22	1	-.34
22	2	3.61
22	3	-.68
22	4	1.50
22	5	-.68
22	6	2.30
22	7	1.42
22	8	-2.78
22	9	-.57
22	10	-3.06
22	11	-1.91
22	12	1.23
22	13	.80
22	14	2.02
22	15	1.49
23	0	3.00
23	1	-.83
23	2	3.71
23	3	-.37
23	4	.67
23	5	-.59
23	6	2.67
23	7	1.49
23	8	-3.05
23	9	-.05
23	10	-2.47
23	11	-1.84
23	12	.93
23	13	.61
23	14	1.96
23	15	1.55
24	0	-1.09
24	1	.89
24	2	3.76
24	3	.61
24	4	-1.20
24	5	-1.12
24	6	1.89
24	7	-1.95
24	8	1.51
24	9	-1.20
24	10	-.51
24	11	-.89
24	12	.83
24	13	.27
24	14	-1.37
24	15	.98
25	0	1.55

m	n	I_{mn}
25	1	-1.29
25	2	-4.52
25	3	.37
25	4	-.07
25	5	-2.09
25	6	-2.24
25	7	-.55
25	8	-1.12
25	9	4.69
25	10	2.76
25	11	1.94
25	12	-.36
25	13	-2.00
25	14	-4.16
25	15	1.61
26	0	4.64
26	1	-.56
26	2	-.61
26	3	4.06
26	4	1.77
26	5	-.69
26	6	1.32
26	7	-.25
26	8	1.56
26	9	-2.35
26	10	-3.05
26	11	.14
26	12	.43
26	13	2.26
26	14	-.26
26	15	.03
27	0	-.53
27	1	-.68
27	2	.22
27	3	1.24
27	4	-1.69
27	5	5.73
27	6	-1.36
27	7	.10
27	8	.07
27	9	-.32
27	10	-2.24
27	11	-.79
27	12	1.38
27	13	-.02
27	14	1.07
27	15	2.00
28	0	2.21
28	1	3.81
28	2	1.83
28	3	2.39
28	4	-.98
28	5	-.78
28	6	-3.46
28	7	1.65
28	8	-.39
28	9	5.47
28	10	-4.91
28	11	-.79
28	12	6.66
28	13	-3.11
28	14	-4.11
28	15	.44
29	0	4.73
29	1	5.28
29	2	5.68
29	3	.12
29	4	-4.40
29	5	-2.76
29	6	3.54
29	7	-.12
29	8	-4.70
29	9	3.58
29	10	-.62
29	11	-2.24
29	12	2.69
29	13	-4.56
29	14	3.11
29	15	-1.44

CONCLUSIONS

In this report we have discussed the problem of finding a current or voltage distribution in the vicinity of a vehicle antenna from a knowledge of the system radiation pattern. The object of determining the source distribution is to locate structural features near the antenna having significant effect on the radiation pattern. The reasonable assumption is made that structural features which have high current densities will affect the radiation pattern significantly.

It was shown in the report that for certain source geometries a knowledge of the radiation pattern in amplitude and phase is sufficient to allow a determination of the source distribution. It was also shown that for some types of sources occurring often in practice a knowledge of the pattern amplitude alone enables us to find the source distribution and thus locate obstacles in the vicinity of the antenna.

Several synthesis methods for finding the source distribution from the radiation pattern were discussed. Many of the methods were adapted to the obstacle-location problem from the pattern-synthesis studies of other researchers. Some methods of synthesis were developed by the present authors and applied to the obstacle-location problem. Source geometries considered were linear, circular, rectangular planar, and cylindrical. The methods used ranged from the simple Fourier series study of straight-line sources to such a highly complex method as the Gram-Schmidt orthogonalization procedure.

The linear Fourier series method was applied to measured radiation patterns of a slot on a finite ground plane with obstacles placed on the plane. Considerable success was achieved in locating the obstacles from the pattern.

The FORTRAN program for this method is given in an appendix. The Woodward method for a linear source was also applied to the pattern calculated from a known linear distribution, and reproduction of the source distribution was excellent. A method of Ksienski was applied to the calculated two-dimensional pattern of a cylindrical source and was found to work reasonably well in determining the cylindrical source distribution. This method is not highly recommended, however, because of inherent errors. The authors have developed a synthesis method for the cylindrical source which is felt to be superior to Ksienski's method.

In conclusion, it is felt that the methods developed and utilized in this report provide a highly useful and practical means for locating pattern-disturbing structures near an antenna.

REFERENCES

1. R. F. Harrington, "Time-Harmonic Electromagnetic Fields," McGraw-Hill Book Company, Inc., New York, N. Y., 1961, p. 106.

2. Harrington, op. cit, p. 100.

3. E. T. Whittaker and G. N. Watson, "A Course of Modern Analysis," University Press, Cambridge, 1962, pp. 219-223.

4. F. R. Gantmacher, "The Theory of Matrices," Vol. I, Chelsea Publishing Co., New York, N. Y., 1960, p. 256.

5. A. Ksienski, "Synthesis of Antenna Radiation Patterns from Discrete Sources," Ph.D. Dissertation at University of Southern California, Los Angelis, California, 1958, pp. 133-134.

6. Gantmacher, op. cit, pp. 23-27.

7. C. H. Walter , "Traveling Wave Antennas," McGraw-Hill Book Company, New York, N. Y., 1965, pp. 95-99.

8. H. F. Davis, "Fourier Series and Orthogonal Functions," Allyn and Bacon, Inc., Boston, 1963, pp. 76, 113-118.

9. W. Magnus and F. Oberhettinger, "Formulas and Theorems for the Functions of Mathematical Physics," Chelsea Publishing Co., New York, N. Y., 1949, p. 30.

10. Whittaker and Watson, op. cit, pp. 15-30.

APPENDIX

FORTRAN PROGRAM FOR LINEAR ARRAY - FOURIER SERIES METHOD

Program evaluates the coefficients in the series

$$E(\theta) = \sum_{-M}^{M} I_m e^{im\beta d_x \cos\theta}$$

by numerical integration over the range $\theta = 0$ to $180°$ for $\beta d_x = \pi$ radians $(d_x = \frac{\lambda}{2})$

$$I_m = \frac{-1}{2\pi} \int_o^{\pi} E(\theta) e^{-im\pi \cos\theta} d(\cos\theta) \approx \frac{1}{2\pi} \sum_{i=o}^{2M} E(\theta_i) e^{-im\pi \cos\theta_i} (\cos\theta_{i+1} - \cos\theta_i)$$

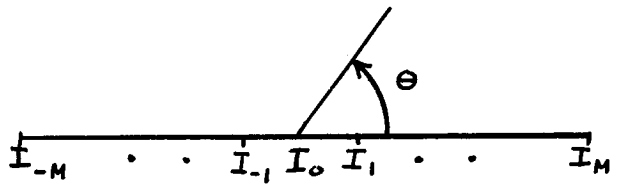

INPUT DATA (must be put on data cards)

1. M = upper limit to summation
2. BL = βd_x in degrees (best choice is 180°)
3. DELTA = 0°
4. FREQ = frequency in Gc.
5. DB(I) = field magnitude measured in db. (need 91 data points taken in two degree increments)

The FORTRAN format statements for the above inputs are:

```
      READ 1,M,BL,DELTA,FREQ
1     FORMAT (I4,2F6.2,F7.4)
      READ 55, (DB(I),I=1,91)
55    FORMAT (20F4.1)  <------ This could be altered if greater
                               accuracy is required.
```

OUTPUT

1. Field magnitudes after conversion from db.
2. The values of M,BL,DELTA, and FREQ
3. The array elements: real and imaginary parts, magnitude and phase, and their distance from the center element in centimeters and feet.
4. Regenerated field.

FORTRAN PROGRAM FOR LINEAR ARRAY

```
' FOR MAIN
C       READ M,BL,DELTA,AND FREQ.  (BL AND DELTA IN DEGREES,FREQ. IN GC.)
        READ 1,M,BL,DELTA,FREQ
     1  FORMAT (I4,2F6.2,F7.4)
        SEP=BL/(12.0*FREQ)
C       READ DATA IN DB. TAKEN IN 2 DEGREE INCREMENTS
        DIMENSION DB(91)
        READ 55, (DB(I),I=1,91)
    55  FORMAT (20F4.1)
C       CONVERT DATA FROM DB.
        CONST=(ALOG(10.0))/20.0
        DIMENSION FNTH(91)
        DO 6 I=1,91
     6  FNTH(I)=EXP(DB(I)*CONST)
C       PRINT PATTERN POINTS (FNTH)
        PRINT 7,
     70FORMAT (35H E-FIELD PATTERN POINTS FOR PATTERN//56H THETA
      1       E            THETA                    E)
        J=0
        DO 9  I=1,45
        K=I+46
        L=J+92
        PRINT 8, J,FNTH(I),L,FNTH(K)
     8  FORMAT (1XI3,F20.3,11XI3,F20.3)
     9  J=J+2
        PRINT 2,J,FNTH(46)
     2  FORMAT (1X,I3,F20.3,////////////////////)
C       PRINT ARRAY
    41  FORMAT (35X17HARRAY FOR PATTERN,//)
        PRINT 41,
    42  FORMAT (3H M=I4,10X3HBL=F6.2,12X6HDELTA=F6.2,10X5HFREQ=F7.4,2HGC)
        PRINT 42,M,BL,DELTA,FREQ
    43  FORMAT ( 100H SOURCE   DISTANCE FROM CENTER          REAL
      1 IMAGINARY          MAGNITUDE               ANGLE )
        PRINT 43,
    44  FORMAT ( 26H           CM           FEET)
        PRINT 44,
C       CONVERT 90 DATA PTS TO 2MAX DATA PTS
        MAX=M+1
        DIMENSION E(1602),PSI(1602)
        DIMENSION P(801),Q(801)
        DIMENSION AMAG(801),ANGLE(801)
        MUD=2*MAX
        SPACES=0.0
        SPACES=(2.0*MAX-1.0)/90.0
        I=1
        DO 19 N=1,MUD
        IF (N-1.0-I*SPACES) 22,23,23
    23  I=I+1
    22  SLOPE=FNTH(I+1)-FNTH(I)
        E(N)=FNTH(I)+SLOPE*((N-1.0)/SPACES+1.0-I)
    19  PSI(N)=BL*COS((N-1.0)*3.141593/(MUD-1.0))/57.296
        DO 20 K=1,MAX
```

```
      P(K)=0.0
      Q(K)=0.0
      MDEL=MUD-1
      DO 21 I=1,MDEL
      P(K)=P(K)+(E    (I)*COS(FLOAT(K-1)*PSI(I))+E    (I+1)*COS(FLOAT(K-1)
     1*PSI(I+1)))*(ABS(PSI(I+1)-PSI(I)))*57.296/720.0
  210Q(K)=Q(K)+(E    (I)*SIN(FLOAT(K-1)*PSI(I))+E    (I+1)*SIN(FLOAT(K-1)
     1*PSI(I+1)))*(ABS(PSI(I+1)-PSI(I)))*57.296/720.0
      AMAG(K)=SQRT(ABS((P(K))**2+(Q(K))**2))
      ANGLE(K)=0.0
      ANGLE(K)=ATAN(Q(K)/(P(K)+1.0E-5))
      ANGLE(K)=ANGLE(K)*57.296
      CM=FLOAT(K-1)*SEP
      FT=CM/30.48
      PRINT 20,K,CM,FT,P(K),Q(K),AMAG(K),ANGLE(K)
   20 FORMAT (1XI4,2F12.3,4F19.6)
      PRINT 300,
  300 FORMAT (1H1)
C     PATTERN REGENERATION FROM ARRAY
C     CALCULATE PATTERN POINTS  (F)
      DIMENSION F(1000)
      DO 5 I=1,MUD
      F(I)=0.0
      DO 4 K=2,MAX
    4 F(I)=F(I)+2.0*P (K)*COS(PSI(I)*FLOAT(K-1))
      F(I)=F(I)+P(1)
      DO 5 K=2,MAX
    5 F(I)=F(I)+2.0*Q (K)*SIN(PSI(I)*FLOAT(K-1))
C     CALCULATE POINTS IN DB.
      DO 66 I=1,MUD
      DB(I)=8.68*ALOG(ABS(F(I)))
      PRINT 100,I,DB(I)
   66 CONTINUE
  100 FORMAT (1XI4 ,1F20.6)
      STOP
      END
' XQT MAIN/CODE
```